

# A unified diagnostic test for regression discontinuity designs\*

Koki Fusejima,<sup>†</sup> Takuya Ishihara,<sup>‡</sup> and Masayuki Sawada<sup>§</sup>

## Abstract

Diagnostic tests for regression discontinuity design face a size-control problem. We document a massive over-rejection of the identifying restriction among empirical studies in the top five economics journals. At least one diagnostic test was rejected for 21 out of 60 studies, whereas less than 5% of the collected 799 tests rejected the null hypotheses. In other words, more than one-third of the studies rejected at least one of their diagnostic tests, whereas their underlying identifying restrictions appear valid. Multiple testing causes this problem because the median number of tests per study was as high as 12. Therefore, we offer unified tests to overcome the size-control problem. Our procedure is based on the new joint asymptotic normality of local polynomial mean and density estimates. In simulation studies, our unified tests outperformed the Bonferroni correction. We implement the procedure as an R package `rdtest` with two empirical examples in its vignettes.

---

\*The study was supported by JSPS KAKENHI Grant Numbers JP20J20046, JP23K18799 (Fusejima), JP22K13373 (Ishihara), and JP21K13269 (Sawada). This study is derived from a chapter of Koki Fusejima's dissertation. We thank Eiji Kurozumi, Yukitoshi Matsushita, Katsumi Shimotsu, and Kohei Yata, as well as seminar participants at Hitotsubashi University, The University of Tokyo, Kansai Keiryo Keizaigaku Kenkyukai, Japanese Joint Statistical Meeting, International Conference on Econometrics and Statistics, and the Asian Meeting of the Econometric Society in East and South-East Asia. Moreover, we thank Masaki Oguni and Yuri Sugiyama for their excellent research assistance. This version: July 23, 2024

<sup>†</sup>Hitotsubashi Institute for Advanced Study, Hitotsubashi University; k.fusejima@r.hit-u.ac.jp

<sup>‡</sup>Graduate School of Economics and Management, Tohoku University; takuya.ishihara.b7@tohoku.ac.jp

<sup>§</sup>Institute of Economic Research, Hitotsubashi University; m-sawada@ier.hit-u.ac.jp

# 1 Introduction

Diagnostic tests are vital to regression discontinuity (RD) design. The typical procedure evaluates the testable restrictions implied by a non-testable identifying restriction, *local randomization*.<sup>1</sup> Local randomization implies identification (Hahn, Todd, and der Klaauw, 2001) and testable restrictions for density and conditional expectation functions (Lee, 2008). All such testable restrictions must hold whenever identification is expected via local randomization. Hence, one must test the null hypothesis of *all restrictions hold* against the alternative hypothesis of *at least one restriction fails*.

However, these restrictions are often tested separately without appropriate size control. Most empirical studies test these restrictions as null hypotheses for the density test (McCrary, 2008) and the balance or placebo test (Lee, 2008; Lee and Lemieux, 2010). These tests are well-established separately but are rarely evaluated jointly. Hence, the multiple-testing problem plagues size control. Consequently, empirical studies may over-reject the underlying null hypothesis that all restrictions hold under local randomization.

In this study, we document the severe over-rejection of the underlying identification restriction in a meta-analysis of 60 empirical RD studies published recently in the top five economics journals.<sup>2</sup> We found that 21 out of 60 studies rejected at least one testable restriction, leading to the underlying restriction being rejected in 35% of the studies.

Nevertheless, each test appeared valid. Among 799 tests run separately, only 4.6% of the restrictions were rejected, and their p-values uniformly distributed over  $[0, 1]$ , suggesting that the test statistics are drawn from the null hypothesis that all testable restrictions hold. Hence, the underlying local randomization was valid; nonetheless, we ended up with an incorrect conclusion for 21 studies rather than three.

We conclude that this over-rejection was caused by multiple testing problems. In 60 studies, the median number of tests was 12 per study. Furthermore, we found only five studies out of 60 reporting some type of joint testing. No study has reported a

---

<sup>1</sup>We refer to Lee (2008) for local randomization. This concept is also known as the continuity-based approach (Cattaneo, Idrobo, and Titiunik, 2019), whereas the term local randomization may be reserved for a stronger restriction for finite sample analysis in which explicit randomization is considered within a small range (Cattaneo, Frandsen, and Titiunik, 2015; Cattaneo, Titiunik, and Vazquez-Bare, 2016, for example).

<sup>2</sup>See Appendix B for the search criterion.

joint test that combines the density and balance or placebo tests because no test has been proposed to handle them jointly.

In this study, we propose a unified diagnostic test to resolve this over-rejection problem. This involves two major challenges. First, no tests consider the joint nature of the density and balance tests. Second, the test statistics are nonparametric estimates. Only one of the five studies considered the nonparametric nature of the test statistics. To address these two challenges, we derived the joint asymptotic normality of the nonparametric density estimation and nonparametric conditional mean estimation. We find that nonparametric density estimates and conditional mean estimates are asymptotically orthogonal. Based on this finding, we provide the first unified test with density and balance test statistics based on our new theoretical results from their nonparametric bias-corrected estimates.

Our unified test aggregates the vector of the density and balance test statistics; however, possible aggregation is not unique. An appropriate aggregation depends on the underlying alternative hypothesis. We considered two different aggregations: (1) a Wald (chi-squared) statistic of the sum of the squared statistics of the vector and (2) a Max test statistic of the maximum squared statistics of the vector. The two test statistics complement each other in detecting different types of alternative hypotheses.

The Wald statistic detects the alternative hypothesis that a large fraction of the original vector deviates from the null hypothesis. The Max statistic detects the alternative hypothesis that only a small fraction of the vector deviates from the null hypothesis. Nevertheless, the conventional Wald statistic did not attain the nominal size, possibly because of poor inverse estimation of the variance matrix. We bypass this problem by standardizing and calculating the squared sum and propose it as the *standardized* Wald (hereafter, sWald) statistic.

In numerical simulations, the sWald and Max statistics exhibit appropriate size control properties for a moderate number of covariates when the sample size is as large as 1000. In particular, the sWald test is superior to other methods in size control performance for any number of covariates up to 25 in cases where even the Bonferroni correction may fail to achieve size control. <sup>3</sup>

We verified the superior power properties of the proposed methods. The Max test

---

<sup>3</sup>We conjecture that the reason for this failure is that Bonferroni correction with 25 covariates evaluates the thin tail of the nonparametric test statistic distribution, which could be imprecisely estimated.

is superior to the Bonferroni correction in its power against the alternative hypothesis that only one covariate sees a jump in the conditional mean. The sWald test is superior to the Bonferroni correction in its power against the alternative hypothesis that all covariates see jumps in their conditional means. In conclusion, we recommend the Max test if a user has a few particularly concerning covariates. Otherwise, we recommend the sWald test for better size control and power in other scenarios.

This study contributes to the literature on diagnostic procedures for RD design.<sup>4</sup> McCrary (2008) has developed the density test, and Lee (2008) has concluded that the null hypotheses of the density and balance or placebo tests are the consequences of his local randomization concept. Several theoretical studies have improved these procedures. Otsu, Xu, and Matsushita (2013) have proposed an empirical likelihood-based density test, Cattaneo, Jansson, and Ma (2020) have considered a test based on a local polynomial estimation of the density function, and Bugni and Canay (2021) have proposed an approximate sign test for the density test. Nevertheless, none of these studies have considered the joint procedure for these tests. Diagnostic test practices follow a similar pattern: separate multiple testing of these diagnostic tests or some joint procedure without considering the nonparametric nature of the test statistics. In this study, we provide unified testing for the single identifying restriction that implies the null hypotheses of these diagnostic tests. We also provide a statistical software *rdtest*, which is an explicit wrapper of two standard packages, *rdrobust* (Calonico, Cattaneo, Farrell, and Titiunik, 2017) and *rddensity* (Cattaneo, Jansson, and Ma, 2018). Therefore, we provide an easy-to-implement unified diagnostic procedure for local randomization based on widely used procedures.

Our study is particularly related to Canay and Kamat (2018), who have delivered a balance test in distribution functions with an extension for joint testing among balance tests. Our procedure is based on the widely used test statistics that are asymptotically valid, with well-maintained packages for density and balance or placebo tests. In comparison, the procedure in Canay and Kamat (2018) is a randomization test that can handle small-sample approaches, such as the latest alternative RD strategy under a substantially stronger but explicit assumption of local randomization (Cattaneo et al., 2015 and Cattaneo et al., 2016). Furthermore, our meta-analysis confirms the critical nature of the multiple-testing problem in the RD diagnostic context, and

---

<sup>4</sup>For an extensive survey of RD literature, see Imbens and Lemieux (2008), Lee and Lemieux (2010), DiNardo and Lee (2011), and Cattaneo et al. (2019,2023)

our simulation evidence deepens our understanding of the vector of test statistics. Consequently, we add to Canay and Kamat (2018) by offering a complementary testing procedure and demonstrating the need for a unified testing procedure in the diagnostics of RD designs.

Moreover, we contribute to the asymptotic theory of nonparametric estimates. We show the joint asymptotic normality of multiple local polynomial estimates for the conditional mean and density functions. Calonico, Cattaneo, and Titiunik (2014) show the asymptotic normality of a single local polynomial estimate for a conditional mean function at a boundary point after bias correction. Cattaneo et al. (2020) also show the asymptotic normality of a local polynomial estimate of a density function at a boundary point. We developed the joint normality results based on these results. Nevertheless, no restrictions are imposed on the choice of bandwidth apart from the original rate conditions. Consequently, we succeeded in accommodating the same mean squared error (MSE) optimal estimates for the balance and placebo tests (Calonico et al., 2014)<sup>5</sup> and density tests (Cattaneo et al., 2020).

The remainder of the paper proceeds as follows. Section 2 demonstrates the multiple testing problem in the meta-analysis, and Section 3.1 explains the joint asymptotic normality of the nonparametric estimates. Subsequently, Section 3.2 presents our joint tests, and Section 4 demonstrates the performance of our tests in the simulation. Finally, Section 5 concludes the article by recommending practices and proposing future research questions. In Appendix A, we provide all the formal results and the proofs.

## 2 Current practices of diagnostic tests

Most empirical studies diagnose their designs using two continuity restrictions: the density function of the running variable and the conditional mean functions of the

---

<sup>5</sup>Recently, another bandwidth selector of coverage error optimal bandwidths has been proposed by Calonico, Cattaneo, and Farrell (2020) along with theoretical background Calonico, Cattaneo, and Farrell (2022). In our numerical analyses and implementation, we used the default option for MSE optimal bandwidths.

pretreatment covariates.<sup>6</sup> These restrictions are necessary<sup>7</sup> for local randomization (Lee, 2008) that implies the *continuity* condition (Hahn et al., 2001) for identification. The logic behind the diagnoses is as follows. If we claim identification via local randomization, all testable continuity restrictions should hold, and none of them must be violated. Hence, we must test the null hypothesis that *all testable restrictions hold* against the alternative hypothesis that *at least one restriction fails* to diagnose the underlying designs.

However, most studies have tested these restrictions separately as density tests (McCrary, 2008; Cattaneo et al., 2020, for example) and balance or placebo tests (Lee, 2008; Lee and Lemieux, 2010, for example). Running these tests separately would over-reject the underlying null hypothesis that all testable restrictions hold because of the multiple testing problem.

We quantified the size control problem by conducting a meta-analysis of RD studies published in the top five economics journals. Among 60 papers that satisfied our search criteria up to November 2021, we collected 799 reported test statistics.<sup>8</sup> Our meta-analysis found two facts: (1) the reported test statistics appear to conform to the null hypothesis that all restrictions hold; (2) nonetheless, 35% (21) studies had at least one rejected test.

## 2.1 Fact 1: Test statistics are likely drawn from the null distributions

First, we document the reported test statistics likely to be drawn from null distributions. Table 2 presents the percentage of tests rejected from the reported ones. Among 799

---

<sup>6</sup>There are other popular diagnoses such as the *placebo cutoff* analysis. In this study, we focus on the practices that are direct implications of the local randomization assumption in Lee (2008). See Cattaneo et al. (2019, Section 5) for further diagnostic concepts.

<sup>7</sup>Importantly, no direct connection exists between the diagnostic restrictions and point identification. For example, the density test is neither necessary nor sufficient for identification (McCrary, 2008). See Ishihara and Sawada (2023) for conditions under which the null hypothesis of the density test implies point identification.

<sup>8</sup>Many studies aim to demonstrate their robustness with different specifications of the same tests with different bandwidths, order of polynomials, or kernels. We screen the *main* specification for each test, and our reported results are the lower bounds of their over-rejections. See Appendix B for details.

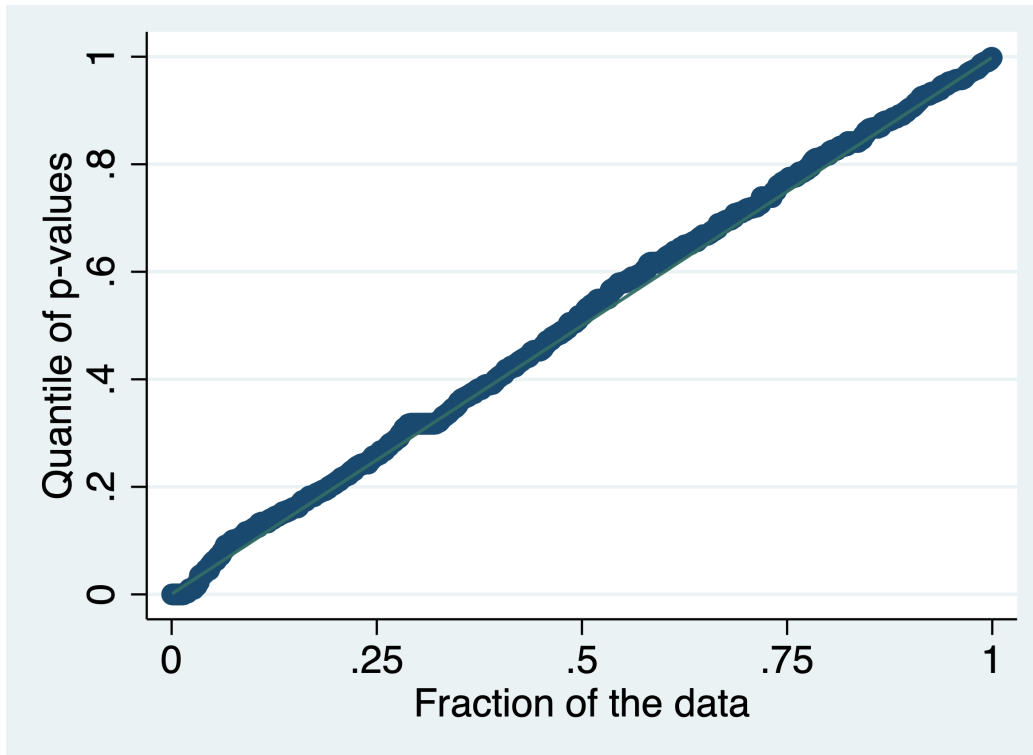
tests reported in 60 studies, we found that less than 5% rejected null hypotheses. Figure 1 shows the quantile plot of the p-values. The quantile plot aligns with the 45-degree line, and the distribution is likely to be uniform over  $[0, 1]$ . Both lines of evidence support the null hypothesis that all restrictions hold under local randomization.

Table 1: Percentage of rejected tests

	Balance	Density	Total
Rejected	4.64%	4.35%	4.63%
Not	95.36%	95.65%	95.37%
Number of tests	776	23	799

*Notes:* Percentages of tests reported as *rejected* and *non-rejected* among 776 balance tests, 23 density tests, and 799 tests in total. See Appendix B for details.

Figure 1: Quantile plot of p-values of tests



*Notes:* The quantile plot of p-values that are reported or computed from t-statistics. Plot aligned with the solid 45 degree line implies similarity to the uniform distribution over  $[0, 1]$ .

## 2.2 Fact 2: The underlying null hypothesis is over-rejected because of multiple testing

From Fact 1, approximately three studies out of 60 should have shown any test rejection because the null hypotheses appear valid. However, Table 2 suggests that 35% of the studies (21 of 60) rejected at least one null hypothesis. As shown in Table 2 and Figure 2, many studies ran more than 10 diagnostic tests without appropriate size control. Hence, we blame the multiple testing problem for over-rejecting the null hypothesis of *all restrictions hold*.

Notably, only five studies reported joint testing for balance tests. All but one study did not consider the nonparametric nature of the test statistics.<sup>9</sup> Furthermore, no studies have reported joint testing of the balance and density tests because no method is available for the joint test. Hence, we propose the following method.

Table 2: Fraction of rejecting at least one hypothesis.

	mean	median	sd
Number of tests per study	14.17	12	9.51
Fraction rejecting at least one test	0.35	-	0.48
Number of rejected tests per study	0.75	0	1.54
Number of studies	60		

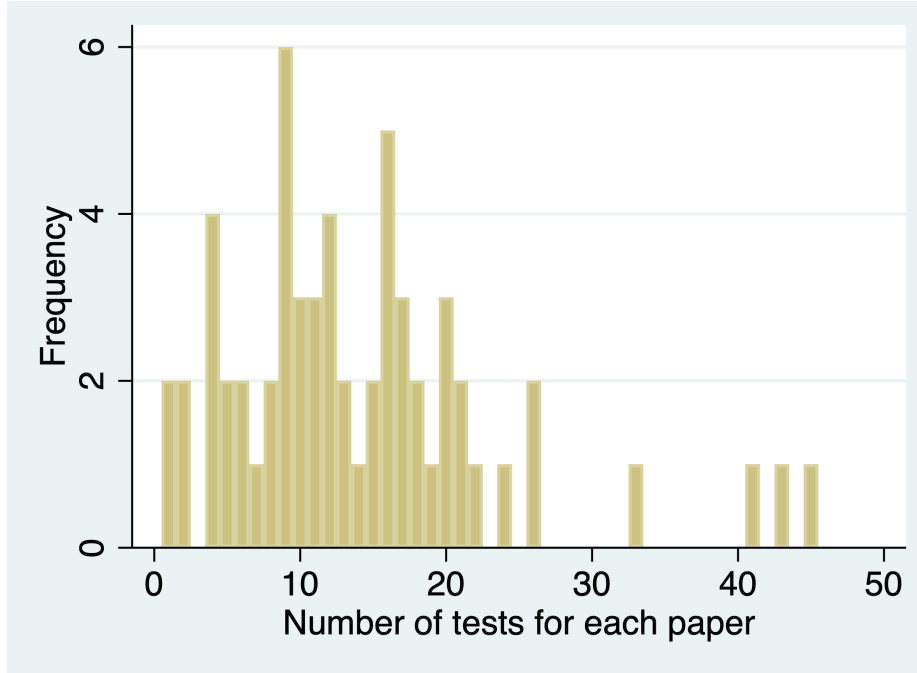
*Notes:* The table shows the mean, median, and standard deviation for the number of tests per study, the fraction of rejecting at least one test per study, and the number of rejected tests per study out of 60 studies.

---

<sup>9</sup>We confirm some sort of joint testing in the following five studies: Meyersson (2014); Abdulkadiroğlu, Angrist, and Pathak (2014); Johnson (2020); Fort, Ichino, and Zanella (2020). Fort et al. (2020) use a nonparametric procedure by Canay and Kamat (2018).



Figure 2: Histogram of the number of tests



*Notes:* This figure is the histogram of the number of tests reported in each study.

### 3 Unified test based on joint asymptotic normality

As shown in Section 2, the multiple-testing problem causes the over-rejection of the underlying identification restriction. We introduce a notation to formally state the problem. Let  $(Z_{1,i}, \dots, Z_{d,i}, X_i)'$ ,  $i = 1, \dots, n$  denote the observed random sample, where  $X_i$  is the running variable with density  $f(x)$  with respect to the Lebesgue measure and  $Z_i = (Z_{1,i}, \dots, Z_{d,i})'$  denote the pre-treatment covariates. Given a known threshold  $\bar{x}$ , which we set to  $\bar{x} = 0$  without loss of generality, let the running variable  $X_i$  determine whether unit  $i$  is assigned a treatment ( $X_i \geq 0$ ) against ( $X_i < 0$ ). In this notation, the local randomization (Lee, 2008) implies identification via Hahn et al. (2001) and two different types of restrictions: the density function  $f(x)$  is continuous at  $x = 0$ , and the conditional mean functions of  $Z_k$ ,  $\mu_{Z_k}(x) = E[Z_{k,i}|X_i = x]$  for  $k = 1, \dots, d$ , are continuous at  $x = 0$ . Specifically, the following  $d + 1$  restrictions must

hold simultaneously

$$f_+ = f_-, \mu_{Z_1+} = \mu_{Z_1-}, \dots, \mu_{Z_d+} = \mu_{Z_d-}$$

where  $f_+ = \lim_{x \rightarrow 0^+} f(x)$ ,  $f_- = \lim_{x \rightarrow 0^-} f(x)$  and  $\mu_{Z_k+} = \lim_{x \rightarrow 0^+} \mu_{Z_k}(x)$ ,  $\mu_{Z_k-} = \lim_{x \rightarrow 0^-} \mu_{Z_k}(x)$ . Hence, one must conduct the following test:

$$H_0 : (\tau_f, \tau_{Z_1}, \dots, \tau_{Z_d}) = 0 \quad \text{vs} \quad H_1 : (\tau_f, \tau_{Z_1}, \dots, \tau_{Z_d}) \neq 0,$$

to determine whether identification via local randomization is valid where  $\tau_f = f_+ - f_-$  and  $\tau_{Z_k} = \mu_{Z_k+} - \mu_{Z_k-}$ . However, if one runs  $d + 1$  tests separately:

$$\begin{aligned} H_{0f} : \tau_f = 0 & \quad \text{vs} \quad H_{1f} : \tau_f \neq 0, \\ H_{01} : \tau_{Z_1} = 0 & \quad \text{vs} \quad H_{11} : \tau_{Z_1} \neq 0, \\ & \quad \vdots \\ H_{0d} : \tau_{Z_d} = 0 & \quad \text{vs} \quad H_{1d} : \tau_{Z_d} \neq 0, \end{aligned}$$

the null hypothesis  $H_0$  are over-rejected as documented in Section 2.

We resolved the size control problem by presenting a unified test in two steps. First, we present the theoretical basis for our unified test. Second, we propose two test statistics for the unified test against multiple testing.

### 3.1 New joint normality result

First, we derive the joint asymptotic normality of the nonparametric local polynomial estimators for  $f$  and  $(\mu_{Z_1}, \dots, \mu_{Z_d})$  evaluated at the boundary of the support.

Following Calonico et al. (2014) and Cattaneo et al. (2020), we use local polynomial regressions to approximate the unknown functions  $f(x)$  and  $\mu_{Z_k}(x)$  for  $k = 1, \dots, d$  flexibly near the cutoff  $\bar{x} = 0$ ; see Fan and Gijbels (1996) for a review of local polynomial regressions. Based on the testing problem, we must obtain two distinct estimands for each function using the two subsamples  $\{X_i : X_i \geq 0\}$  (approximation from the right) and  $\{X_i : X_i < 0\}$  (approximation from the left) at a boundary point  $x = 0$ . These estimators are recommended owing to their excellent boundary properties.

Using a polynomial expansion, we construct smooth local one-sided approximations of the sample average of  $Z_{k,i}$  and obtain the estimators  $\hat{\mu}_{Z_k+,l}(h_{k,n})$  and  $\hat{\mu}_{Z_k-,l}(h_{k,n})$  as intercepts in the local polynomial regression. Specifically, we estimate  $\tau_{Z_k}$  using the following  $l$ th-order local polynomial estimators: for some  $l \geq 1$  and for each

$k = 1, \dots, d,$

$$\hat{\tau}_{Z_k, l}(h_{k, n}) = \hat{\mu}_{Z_k+, l}(h_{k, n}) - \hat{\mu}_{Z_k-, l}(h_{k, n}),$$

$$\hat{\mu}_{Z_k+, l}(h_{k, n}) = e'_0 \hat{\beta}_{Z_k+, l}(h_{k, n}), \quad (3.1)$$

$$\hat{\mu}_{Z_k-, l}(h_{k, n}) = e'_0 \hat{\beta}_{Z_k-, l}(h_{k, n}), \quad (3.2)$$

where

$$\hat{\beta}_{Z_k+, l}(h_{k, n}) = \arg \min_{\beta \in \mathbb{R}^{l+1}} \sum_{i=1}^n 1\{X_i \geq 0\} (Z_{k, i} - r_l(X_i)' \beta)^2 K(X_i/h_{k, n})/h_{k, n}, \quad (3.3)$$

$$\hat{\beta}_{Z_k-, l}(h_{k, n}) = \arg \min_{\beta \in \mathbb{R}^{l+1}} \sum_{i=1}^n 1\{X_i < 0\} (Z_{k, i} - r_l(X_i)' \beta)^2 K(X_i/h_{k, n})/h_{k, n}, \quad (3.4)$$

$e_0 = (1, 0, \dots, 0)'$  is the first  $(l+1)$ -dimensional unit vector,  $r_l(x) = (1, x, \dots, x^l)'$  is a  $l$ th order polynomial expansion,  $K(\cdot)$  is a kernel function, and  $h_{k, n}$  is a positive-bandwidth sequence.

Similarly, using a polynomial expansion, we construct smooth local one-sided approximations of the empirical distribution of  $X_i$  and obtain the estimators  $\hat{f}_{+, p}(h_{f, n})$  and  $\hat{f}_{-, p}(h_{f, n})$  as the slope coefficients in the local polynomial regression. Specifically, we estimate  $\tau_f$  using the following  $p$ th-order local polynomial estimator. For some  $p \geq 2$ ,

$$\hat{\tau}_{f, p}(h_{f, n}) = \hat{f}_{+, p}(h_{f, n}) - \hat{f}_{-, p}(h_{f, n}),$$

$$\hat{f}_{+, p}(h_{f, n}) = e'_1 \hat{\beta}_{f+, p}(h_{f, n}), \quad (3.5)$$

$$\hat{f}_{-, p}(h_{f, n}) = e'_1 \hat{\beta}_{f-, p}(h_{f, n}), \quad (3.6)$$

where

$$\hat{\beta}_{f+, p}(h_{f, n}) = \arg \min_{\beta \in \mathbb{R}^{p+1}} \sum_{i=1}^n 1\{X_i \geq 0\} (\tilde{F}(X_i) - r_p(X_i)' \beta)^2 K(X_i/h_{f, n})/h_{f, n}, \quad (3.7)$$

$$\hat{\beta}_{f-, p}(h_{f, n}) = \arg \min_{\beta \in \mathbb{R}^{p+1}} \sum_{i=1}^n 1\{X_i < 0\} (\tilde{F}(X_i) - r_p(X_i)' \beta)^2 K(X_i/h_{f, n})/h_{f, n}, \quad (3.8)$$

$e_1 = (0, 1, 0, \dots, 0)'$  is the second  $(p+1)$ -dimensional unit vector;  $\tilde{F}(x) \equiv n^{-1} \sum_{i=1}^n 1\{X_i \leq x\}$  is the empirical distribution function of  $X_i$ , and  $h_{f, n}$  is the positive-bandwidth sequence.

We derive the asymptotic distributions of the local polynomial estimators based on the assumptions in Calonico et al. (2014) and Cattaneo et al. (2020), as follows.

**Assumption 1.** For some  $\kappa_0 > 0$ , the following holds true for  $(-\kappa_0, 0) \cup (0, \kappa_0)$  around the cutoff  $\bar{x} = 0$ .

- (a)  $f(x)$  is  $R$  times continuously differentiable for some  $R \geq 1$  and bounded away from zero.
- (b) For  $k = 1, \dots, d$ ,  $\mu_{Z_k}(x)$  is  $S$  times continuously differentiable for some  $S \geq 1$ ,  $\text{Var}(Z_{k,i}|X_i = x)$  is continuous and bounded away from zero, and  $E[|Z_{k,i}|^4|X_i = x]$  is bounded.

Assumption 1 is a set of basic regularity conditions for the data generation process. Assumption 1 (a) ensures that the density of the running variable is well defined and sufficiently smooth and that the observed values are arbitrarily close to the cutoff for large samples. Assumption 1 (b) ensures that the conditional expectations and variances of the pre-treatment covariates are well defined and have sufficient smoothness with the existence of the fourth moments.

**Assumption 2.** For some  $\kappa > 0$ , the kernel function  $K(\cdot) : \mathbb{R} \rightarrow \mathbb{R}$  is symmetric, bounded, and non-negative; it is zero outside the support, and positive and continuous on  $(-\kappa, \kappa)$ .

Assumption 2 is a set of standard conditions for the kernel function and is satisfied for kernels such as triangular and uniform kernels, commonly used in empirical work. Our results can be extended to accommodate kernels with unbounded supports or asymmetric kernels with more complex notations.

We provide a joint asymptotic distribution for the local polynomial estimators. In the following, let  $l, p \in \mathbb{N}$ ;  $h_n = (h_{1,n}, \dots, h_{d,n})'$ ;  $h_{max,n} = \max\{h_{1,n}, \dots, h_{d,n}\}$ ;  $h_{min,n} = \min\{h_{1,n}, \dots, h_{d,n}\}$ ; we assume that all the limits are  $n \rightarrow \infty$  (and  $h_{k,n}, h_{f,n} \rightarrow 0$ ), unless stated otherwise. Whenever there was no confusion, we dropped the sample size  $n$  sub-index notation. For derivatives  $\mu_{Z_k}^{(s)}(x)$  and  $f^{(s)}(x)$ , let  $\mu_{Z_k+}^{(s)} = \lim_{x \rightarrow 0+} \mu_{Z_k}^{(s)}(x)$ ,  $\mu_{Z_k-}^{(s)} = \lim_{x \rightarrow 0-} \mu_{Z_k}^{(s)}(x)$ ,  $f_+^{(s)} = \lim_{x \rightarrow 0+} f^{(s)}(x)$ , and  $f_-^{(s)} = \lim_{x \rightarrow 0-} f^{(s)}(x)$ .

**Theorem 3.1.** Suppose that Assumptions 1 and 2 hold, with  $R \geq p + 1$  and  $S \geq l + 2$ . If  $nh_{min} \rightarrow \infty$ ,  $nh_f^2 \rightarrow \infty$ ,  $n(h_{max})^{2l+5} \rightarrow 0$  and  $n(h_f)^{2p+3} \rightarrow 0$ , then

$$\sqrt{n} \begin{bmatrix} \sqrt{h_1}(\hat{\tau}_{Z_1,l}(h_1) - \tau_{Z_1} - (h_1)^{1+l}B_{Z_1,l,l+1}(h_1)) \\ \vdots \\ \sqrt{h_d}(\hat{\tau}_{Z_d,l}(h_d) - \tau_{Z_d} - (h_d)^{1+l}B_{Z_d,l,l+1}(h_d)) \\ \sqrt{h_f}(\hat{\tau}_{f,p}(h_f) - \tau_f - h_f^p B_{f,p,p+1}(h_f)) \end{bmatrix} \xrightarrow{d} N_{d+1}(0, V_{l,p}),$$

where  $N_{d+1}(\mu, \Sigma)$  denotes the multivariate normal distribution with  $(d+1)$ -dimensional mean vector  $\mu$  and  $(d+1) \times (d+1)$  covariance matrix  $\Sigma$ ,

$$\begin{aligned} B_{Z^k, l, r}(h_k) &= B_{Z_{k+}, l, r}(h_k) - B_{Z_{k-}, l, r}(h_k) \\ &= \frac{\mu_{Z_{k+}}^{(r)}}{r!} \mathcal{B}_{+, 0, l, r}(h_k) - \frac{\mu_{Z_{k-}}^{(r)}}{r!} \mathcal{B}_{-, 0, l, r}(h_k), \end{aligned}$$

$$\begin{aligned} B_{f, p, q}(h_f) &= B_{f, +, p, q}(h_f) - B_{f, -, p, q}(h_f) \\ &= \frac{f_+^{(q-1)}}{(q-1)!} \mathcal{B}_{+, 1, p, q}(h_f) - \frac{f_-^{(q-1)}}{(q-1)!} \mathcal{B}_{-, 1, p, q}(h_f), \end{aligned}$$

and

$$V_{l, p} = \begin{pmatrix} V_{Z, l} & 0 \\ 0 & V_{f, p} \end{pmatrix}.$$

The exact forms of  $\mathcal{B}_{+, s, l, r}(h)$  and  $\mathcal{B}_{-, s, l, r}(h)$  are provided in Appendix A.2. The exact forms of  $V_{Z, l}$  and  $V_{f, p}$  are provided in Appendix A.4.

Theorem 3.1 shows that the joint asymptotic distribution of  $\hat{\tau}_{f, p}(h_f)$  and  $\hat{\tau}_{Z_k, l}(h_k)$  is a multivariate normal distribution under the same set of conditions as in Calonico et al. (2014) for  $\hat{\tau}_{Z_k, l}(h_k)$  and Cattaneo et al. (2020) for  $\hat{\tau}_{f, p}(h_f)$ . Hence, the proposed joint distributional approximation is a natural generalization of the distributional approximation of each local polynomial estimator in these studies.

We emphasize that the covariance matrix of  $(\hat{\tau}_{Z_1, l}(h_1), \dots, \hat{\tau}_{Z_d, l}(h_d))'$  and the variance of  $\hat{\tau}_{f, p}(h_f)$  are asymptotically orthogonal. Orthogonality simplifies the estimation of the overall asymptotic covariance matrix because the asymptotic covariance of  $\hat{\tau}_{f, p}(h_f)$  and  $\hat{\tau}_{Z_k, l}(h_k)$  are known to be zero. We derive this orthogonality from the well-known fact that  $\text{Cov}(Z_{k, i} - \mu_{Z_k}(X_i), g(X_i)) = 0$  for any function  $g$ .

**Remark 1** (Increasing the polynomial order for bias correction). We use bias-corrected estimators for the following analyses. As highlighted in Calonico et al. (2014) and Cattaneo et al. (2020), bias correction is important for inference. As provided in Appendix A.2,  $\mathcal{B}_{+, s, l, r}(h)$  and  $\mathcal{B}_{-, s, l, r}(h)$  are the observed quantities, and the bias-corrected estimators are constructed by replacing  $\mu_{Z_{k+}}^{(r)}$ ,  $\mu_{Z_{k-}}^{(r)}$ ,  $f_+^{(q-1)}$ , and  $f_-^{(q-1)}$  with their local polynomial estimators. Nevertheless, as shown in Calonico et al. (2014), if the same bandwidth and kernel function are used for estimating  $\mu_{Z_{k+}}^{(r)}$  and  $\mu_{Z_{k-}}^{(r)}$ , the bias-corrected estimator is numerically equivalent to  $\hat{\tau}_{Z_k, l+1}(h_k)$  (with no bias-correction). A bias correction based on similar results has been adopted by Cattaneo et al. (2020) for their local polynomial density estimators. Following their approach,

we implement bias correction by increasing the order of the local polynomial estimators.  
10

**Remark 2** (Bandwidth selection). We allow the bandwidths to differ for each estimator as long as the conditions stated in Theorem 3.1 are satisfied. Hence, we may apply the original data-driven bandwidth selection provided in Calonico et al. (2014) for  $h_1, \dots, h_d$  and Cattaneo et al. (2020) for  $h_f$  to our joint distributional approximation. As described above, we used bias-corrected local polynomial estimators. Specifically,  $h_k$  is the MSE-optimal bandwidth for  $\hat{\tau}_{Z_k,l}(h_k)$ , and  $h_f$  is the MSE-optimal bandwidth for  $\hat{\tau}_{f,p}(h_f)$ . We construct the test statistics based on  $\hat{\tau}_{Z_k,l+1}(h_k)$  and  $\hat{\tau}_{f,p+1}(h_f)$ . The latter implementation via  $\hat{\tau}_{f,p+1}(h_f)$  is the default for *rddensity*, based on Cattaneo et al. (2020).

**Remark 3** (Asymptotic covariance matrix). We estimate the asymptotic covariance matrix as follows.

$$\hat{V}_{l,p}(h) = \begin{pmatrix} \hat{V}_{Z,l}(h) & 0 \\ 0 & \hat{V}_{f,p}(h_f) \end{pmatrix},$$

where

$$\hat{V}_{Z,l}(h) \xrightarrow{P} V_{Z,l}, \quad \hat{V}_{f,p}(h_f) \xrightarrow{P} V_{f,p}.$$

We employed the estimators proposed by Calonico et al. (2014) and Cattaneo et al. (2020) for the asymptotic variances of  $\hat{\tau}_{Z_k,l}(h_k)$  and  $\hat{\tau}_{f,p}(h_f)$  for each diagonal element of the asymptotic covariance matrix  $\hat{V}_{Z,l}(h)$  and  $\hat{V}_{f,p}(h_f)$ . For the covariance estimators of  $\hat{\tau}_{Z_j,l}(h_j)$  and  $\hat{\tau}_{Z_k,l}(h_k)$ , we follow Calonico et al. (2014). Specifically, we propose to estimate the elements of  $\hat{V}_{Z,l}(h)$  based on the nearest-neighbor estimation, which may be more robust than plugging in the corresponding residuals of nonparametric regressions in finite samples. We provide the exact forms of  $\hat{V}_{Z,l}(h)$  and  $\hat{V}_{f,p}(h_f)$  in Appendix A.4.

## 3.2 Proposed unified tests

Given the joint asymptotic normality result, we introduce a unified test for the identifying restriction. We constructed the test statistics based on the bias-corrected local polynomial estimators  $\hat{\tau}_{Z_k,l+1}(h_k)$  and  $\hat{\tau}_{f,p+1}(h_f)$ , where the bandwidth was chosen as MSE-optimal for  $\hat{\tau}_{Z_k,l}(h_k)$  and  $\hat{\tau}_{f,p}(h_f)$ . Our unified test has two forms: one

---

<sup>10</sup>See Appendix A.3 for details.

aggregates the vector of the density and balance test statistics with the  $L^2$ -norm, and the other aggregates them via the  $L^\infty$ -norm.

The Wald (chi-squared) test statistic with the  $L^2$ -norm has the following form.

$$\hat{\chi}_{l+1,p+1}^2(h) = \|(\hat{V}_{l+1,p+1}(h))^{-1/2}\hat{T}_{l+1,p+1}(h)\|_2^2,$$

where

$$\hat{T}_{l,p}(h) = \sqrt{n}[\sqrt{h_1}\hat{\tau}_{Z_1,l}(h_1), \dots, \sqrt{h_d}\hat{\tau}_{Z_d,l}(h_d), \sqrt{h_f}\hat{\tau}_{f,p}(h_f)]'.$$

This conventional test statistic suffers from severe size distortions in finite samples. In particular, the inverse of the asymptotic covariance matrix estimator becomes unstable for a sufficiently large dimension  $d$ .

Instead, we propose a *sWald* test statistic that modifies the Wald test statistic. Specifically, we standardize only the diagonal elements instead of multiplying the entire matrix by the inverse of the asymptotic covariance matrix. The sWald test statistic has the following form:

$$\tilde{\chi}_{l+1,p+1}^2(h) = \|\tilde{T}_{l+1,p+1}(h)\|_2^2,$$

where

$$\tilde{T}_{l,p}(h) = \text{diag}\{(\hat{V}_{Z_1,l}(h))^{-1/2}, \dots, (\hat{V}_{Z_d,l}(h))^{-1/2}, (\hat{V}_{f,p}(h_f))^{-1/2}\}\hat{T}_{l,p}(h),$$

and  $\text{diag}(a_1, \dots, a_n)$  is the  $(n \times n)$  diagonal matrix with diagonal elements  $a_1, \dots, a_n$ .

We obtain the asymptotic distribution of  $\tilde{\chi}_{l+1,p+1}^2(h)$  from the joint asymptotic distribution for the local polynomial estimators, with their diagonal elements standardized by their standard errors  $(\hat{V}_{f,p+1}(h_f))^{1/2}$  and  $(\hat{V}_{Z_k,l+1}(h))^{1/2}$ . We construct the standard errors of  $\tau_{Z_k}$  as  $\hat{V}_{Z_k,l+1}(h) \xrightarrow{P} V_{Z_k,l+1}$ , where  $V_{Z_k,l+1}$  is the asymptotic variance of  $\sqrt{nh_k}(\hat{\tau}_{Z_k,l+1}(h_k) - \tau_{Z_k})$ . The asymptotic covariance matrix of the standardized local polynomial estimators is the asymptotic correlation matrix of the local polynomial estimators for  $\tau_f$  and  $\tau_{Z_k}$ . The correlation matrix  $V_{l+1,p+1}^*$  is

$$V_{l+1,p+1}^* = \begin{pmatrix} V_{Z,l+1}^* & 0 \\ 0 & 1 \end{pmatrix},$$

where  $V_{Z,l}^* = \text{diag}(V_{Z_1,l}^{-1/2}, \dots, V_{Z_d,l}^{-1/2})V_{Z,l}\text{diag}(V_{Z_1,l}^{-1/2}, \dots, V_{Z_d,l}^{-1/2})$ ; our estimator of  $V_{l+1,p+1}^*$  is

$$\hat{V}_{l+1,p+1}^*(h) = \begin{pmatrix} \hat{V}_{Z,l+1}^*(h) & 0 \\ 0 & 1 \end{pmatrix},$$

where

$$\hat{V}_{Z,l}^*(h) = D_{\hat{V}}(h)\hat{V}_{Z,l}(h)D_{\hat{V}}(h) \text{ with } D_{\hat{V}}(h) = \text{diag}\{(\hat{V}_{Z_1,l}(h))^{-1/2}, \dots, (\hat{V}_{Z_d,l}(h))^{-1/2}\}.$$

In the following proposition, we show that the finite-sample distribution of  $\tilde{\chi}_{l+1,p+1}^2(h)$  is approximated by the distribution of the sum of the squares of the  $(d+1)$ -dimensional multivariate normal random vector.

**Proposition 3.1.** *Suppose Assumptions 1 and 2 hold with  $R \geq p+2$  and  $S \geq l+3$ , and the asymptotic variance matrix  $V_{l+1,p+1}$  is nonsingular. If  $nh_{\min} \rightarrow \infty$ ,  $nh_f^2 \rightarrow \infty$ ,  $n(h_{\max})^{2l+5} \rightarrow 0$ , and  $n(h_f)^{2p+3} \rightarrow 0$ , then*

$$\text{Under } H_0 : \lim_{n \rightarrow \infty} P(\tilde{\chi}_{l+1,p+1}^2(h) \geq \hat{c}_{l+1,p+1}(\alpha)) = \alpha,$$

$$\text{Under } H_1 : \lim_{n \rightarrow \infty} P(\tilde{\chi}_{l+1,p+1}^2(h) \geq \hat{c}_{l+1,p+1}(\alpha)) = 1,$$

where  $\hat{c}_{l+1,p+1}(\alpha)$  is the  $(1-\alpha)$ -quantile of the distribution of  $\|N_{d+1}(0, \hat{V}_{l+1,p+1}^*(h))\|_2^2$ .

*Proof.* Let  $c_{l,p}(\alpha)$  be the  $\alpha$ -quantile of  $\|N_{d+1}(0, V_{l,p}^*)\|_2^2$ . Theorem 3.1 implies that  $\tilde{\chi}_{l,p}^2(h) \xrightarrow{d} \|N_{d+1}(0, V_{l,p}^*)\|_2^2$  under  $H_0$ . To prove Proposition 3.1, it suffices to show that  $\hat{c}_{l,p}(\alpha) \xrightarrow{P} c_{l,p}(\alpha)$  because this implies that  $\tilde{\chi}_{l,p}^2(h) - \hat{c}_{l,p}(\alpha) \xrightarrow{d} \|N_{d+1}(0, V_{l,p}^*)\|_2^2 - c_{l,p}(\alpha)$  under  $H_0$ . Let  $F(\cdot; V)$  be the distribution function of  $\|N_{d+1}(0, V)\|_2^2$ . Suppose that  $V_m$  and  $V$  are positive definite matrices for  $m$  and  $V_m \rightarrow V$ . Subsequently, for all  $t \in \mathbb{R}$ , it follows from the dominated convergence theorem that

$$\begin{aligned} F(t; V_m) &= \int \cdots \int 1 \{u_1^2 + \cdots + u_{d+1}^2 \leq t\} \phi(u_1, \dots, u_{d+1}; V_m) du_1 \cdots du_{d+1} \\ &\rightarrow \int \cdots \int 1 \{u_1^2 + \cdots + u_{d+1}^2 \leq t\} \phi(u_1, \dots, u_{d+1}; V) du_1 \cdots du_{d+1} = F(t; V), \end{aligned}$$

where  $\phi(u_1, \dots, u_{d+1}; V)$  denotes the joint density function of  $N_{d+1}(0, V)$ . As  $F(t; V)$  is continuous with respect to  $t$ ,  $F(\cdot; V_m)$  converges uniformly to  $F(\cdot; V)$ , according to Polya's theorem. As discussed in Section 3.9.4.2, in van der Vaart and Wellner (1996), the inverse map is continuous. Thus,  $F^{-1}(\alpha; V_m) \rightarrow F^{-1}(\alpha; V)$  for any  $\alpha \in (0, 1)$ . Hence,  $F^{-1}(t; V)$  is continuous with respect to  $V$ , and we obtain  $\hat{c}_{l,p}(\alpha) \xrightarrow{P} c_{l,p}(\alpha)$  from the continuous-mapping theorem.  $\square$

Proposition 3.1 establishes the asymptotic validity and consistency of the  $\alpha$ -level testing procedure, which rejects  $H_0$  if  $\hat{c}_{l+1,p+1}(\alpha)$  exceeds  $\tilde{\chi}_{l+1,p+1}^2(h)$ . The critical value  $\hat{c}_{l+1,p+1}(\alpha)$  is obtained numerically by generating  $(d+1)$ -dimensional standard normal random vectors using Monte Carlo simulation.



The *Max* test statistic with  $L^\infty$  norm takes the following form.

$$\hat{M}_{l+1,p+1}(h) = \|\tilde{T}_{l+1,p+1}(h)\|_\infty^2.$$

Similar to the sWald statistic, the Max statistic is constructed by standardizing diagonal elements. The following statement shows that the finite sample distribution of  $\hat{M}_{l+1,p+1}(h)$  is approximated by the distribution of the maximum value of the  $(d+1)$ -dimensional multivariate normal random vector.

**Proposition 3.2.** *Suppose Assumptions 1 and 2 hold with  $R \geq p+2$  and  $S \geq l+3$ , and the asymptotic variance matrix  $V_{l+1,p+1}$  is nonsingular. If  $nh_{\min} \rightarrow \infty$ ,  $nh_f^2 \rightarrow \infty$ ,  $n(h_{\max})^{2l+5} \rightarrow 0$  and  $n(h_f)^{2p+3} \rightarrow 0$ ,*

$$\text{Under } H_0 : \lim_{n \rightarrow \infty} P(\hat{M}_{l+1,p+1}(h) \geq \hat{m}_{l+1,p+1}(\alpha)) = \alpha,$$

$$\text{Under } H_1 : \lim_{n \rightarrow \infty} P(\hat{M}_{l+1,p+1}(h) \geq \hat{m}_{l+1,p+1}(\alpha)) = 1,$$

where  $\hat{m}_{l+1,p+1}(\alpha)$  is the  $(1-\alpha)$ -quantile of the distribution  $\|N_{d+1}(0, \hat{V}_{l+1,p+1}^*(h))\|_\infty^2$ .

*Proof.* Proposition 3.2 follows from the same argument as Proposition 3.1.  $\square$

Proposition 3.2 establishes the asymptotic validity and consistency of the  $\alpha$ -level testing procedure, which rejects  $H_0$  if  $\hat{M}_{l+1,p+1}(h)$  exceeds  $\hat{m}_{l+1,p+1}(\alpha)$ . The critical value  $\hat{m}_{l+1,p+1}(\alpha)$  is obtained numerically by generating  $(d+1)$ -dimensional standard normal random vectors using Monte Carlo simulation.

**Remark 4** (Max test against Bonferroni correction). The Max test is more powerful than the Bonferroni correction. The Bonferroni correction conducts asymptotic  $t$  tests separately with an altered size of  $\alpha/(d+1)$ . The Bonferroni correction rejects  $H_0$  if

$$\hat{M}_{l+1,p+1}(h) \geq z^2(\alpha/2(d+1)),$$

where  $z(\alpha/2(d+1))$  is the  $\left(1 - \frac{\alpha}{2(d+1)}\right)$ -quantile of  $N(0, 1)$ , suggesting that the same  $\hat{M}_{l+1,p+1}(h)$  is used for the Bonferroni correction and Max test. For any correlation matrix  $V$ , we obtain

$$P\left(\|N_{d+1}(0, V)\|_\infty^2 \geq z^2(\alpha/2(d+1))\right) \leq \alpha.$$

Furthermore,  $z^2(\alpha/2(d+1))$  must be greater than  $\hat{m}_{l+1,p+1}(\alpha)$  because  $\hat{m}_{l+1,p+1}(\alpha)$  is the  $(1-\alpha)$ -quantile of distribution  $\|N_{d+1}(0, \hat{V}_{l+1,p+1}^*(h))\|_\infty^2$ . Therefore, the rejection probability of the Max test is always higher than that of the Bonferroni correction.

## 4 Simulation evidences for the unified tests

Given the established theoretical properties of the proposed tests, their performance was evaluated using the Monte Carlo experiment. We conducted 3000 replications to generate a random sample  $\{(X_i, Z_{1,i}, \dots, Z_{d,i})' : i = 1, \dots, n\}$  with size  $n = \{500, 1000\}$  for each of them. <sup>11</sup>

We specify the distribution of running variable  $X_i$  as the weighted average of two truncated normal distributions, where  $\bar{p} \geq 0.5$  determines the weights. The density of  $X_i$  is shown in Figure 3. The density  $f(x)$  is continuous at  $x = 0$  if and only if  $\bar{p} = 0.5$  but jumps at  $x = 0$  when  $\bar{p} > 0.5$ .

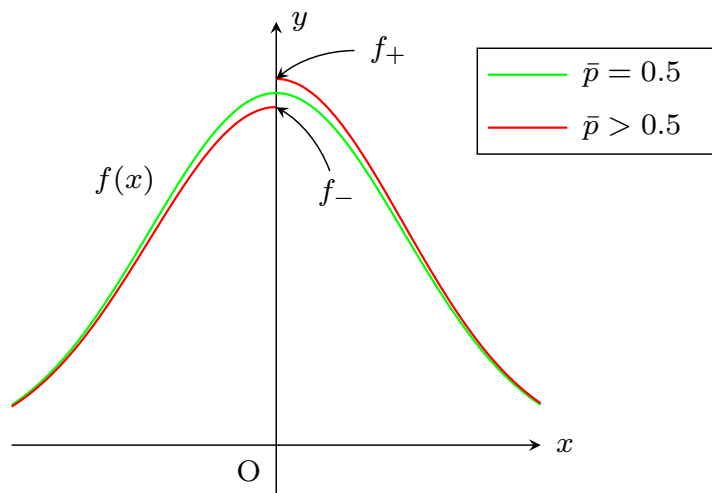


Figure 3: Graph of  $f(x)$

For covariates  $Z_i$ , we consider two specifications: first, one of the  $d$  covariates sees a jump; second, all  $d$  covariates see a jump, with each jump size divided by  $d$ . For the first specification, we have  $\mu_{Z_k}(x) = E[Z_{k,i}|X_i = x]$ ,  $k = 1 \dots, d$  as follows.

$$\mu_{Z_k}(x) = \lambda(x) \text{ for } k = 1, \dots, d-1 \quad \text{and} \quad \mu_{Z_d}(x) = \begin{cases} \lambda(x) & \text{if } x < 0 \\ \lambda(x) + a & \text{if } x \geq 0, \end{cases}$$

where only the  $d$ th covariate sees a jump, and the functional form of  $\lambda(x)$  is obtained from the simulated data close to the data in Lee (2008) following Calonico et al. (2014), where  $a \geq 0$  is the level of discontinuity of  $\mu_{Z_d}(x)$  at  $x = 0$ . For the second

<sup>11</sup>The detailed simulation data generating process is in Appendix C.

specification, we have  $\mu_{Z_k}(x) = E[Z_{k,i}|X_i = x], k = 1, \dots, d$  as follows.

$$\mu_{Z_k}(x) = \begin{cases} \lambda(x) & \text{if } x < 0 \\ \lambda(x) + a/d & \text{if } x \geq 0, \end{cases}$$

where  $a/d$  denotes the discontinuity level for each  $\mu_{Z_k}(x)$  at  $x = 0$ . For both cases, let  $1 > \rho \geq 0$  denote the conditional correlation between  $Z_{j,i}$  and  $Z_{k,i}$ , given  $X_i = x$ . In this data-generating process, the null hypothesis for the joint manipulation test,  $H_0 : (\tau_f, \tau_{Z_1}, \dots, \tau_{Z_d}) = 0$  is true if and only if  $\bar{p} = 0.5$  and  $a = 0$ ;  $\tau_f > 0$  when  $\bar{p} > 0.5$ ;  $\tau_{Z_d} = a > 0$  when  $a > 0$ .

We conducted the tests with size  $\alpha = 0.05$ , employing local polynomial estimators  $(\hat{\tau}_{Z_1,2}(h_1), \dots, \hat{\tau}_{Z_d,2}(h_d), \hat{\tau}_{f,3}(h_f))$  described in Section 3.1 with  $K(u) = (1 - |u|) \vee 0$ , where the bandwidths are chosen to be MSE-optimal for  $\hat{\tau}_{Z_k,1}(h_k)$  and  $\hat{\tau}_{f,2}(h_f)$ . The selection of the kernel function and polynomial order follows Calonico et al. (2014) and Cattaneo et al. (2020).<sup>12</sup> Below, we report the empirical sizes and powers of the conventional and proposed testing methods.

We compared five testing methods: (i) naive testing; (ii) Bonferroni correction of naive testing; (iii) Wald (chi-square) test; (iv) Max test proposed in Section 3.2; (v) sWald test proposed in Section 3.2. Naive testing separately conducts  $d + 1$  asymptotic  $t$  tests, as described in Calonico et al. (2014) and Cattaneo et al. (2020) with a size  $\alpha$  for each of the  $d + 1$  restrictions of the null hypothesis,  $\tau_f = 0, \tau_{Z_1} = 0, \dots, \tau_{Z_d} = 0$ . Naive testing rejects the null hypothesis if at least one test rejects it. The Bonferroni correction conducts asymptotic  $t$  tests separately, but the size is changed to  $\alpha/(d + 1)$  to restrict type 1 error of the null hypothesis that all  $d + 1$  restrictions hold.<sup>13</sup>

In Tables 3–5, we compare the empirical size of each test under the null hypothesis (where  $\bar{p} = 0.5$  and  $a = 0$ ) with different correlation coefficients  $\rho = 0, 0.5, 0.9$ . Notably, naive testing suffers from size distortion, and over-rejection worsens when  $d$  is large. Similarly, the Wald test without correction suffers from size distortion as  $d$  increases. As discussed in Section 3.2, the effective sample size may be too small compared

---

<sup>12</sup>As mentioned in the previous sections, the polynomial orders are chosen so that the estimates are bias-corrected for their valid inference. This choice of polynomial order is the default for *rddensity* and available as  $\rho = 1$  option for *rdrobust*.

<sup>13</sup>We do not benefit from rejecting more than one test for evaluating the underlying identifying restriction. Thus, Holm correction for Bonferroni test does not improve the following results because the probability of rejecting at least one null hypothesis remains the same in two corrections.

to a large  $d$ . When  $d$  is large, the covariance matrix increases, and inverse matrix estimation becomes unstable when the effective sample size is limited.

Table 3: Empirical size of tests (i)–(v) ( $\rho = 0$ )

dim	n: 500					n: 1000				
	naive	bonfe	Wald	Max	sWald	naive	bonfe	Wald	Max	sWald
1	0.095	0.050	0.047	0.060	0.051	0.081	0.035	0.039	0.048	0.046
3	0.185	0.056	0.068	0.064	0.049	0.173	0.049	0.054	0.054	0.043
5	0.289	0.070	0.112	0.077	0.055	0.271	0.052	0.073	0.057	0.044
10	0.464	0.086	0.271	0.088	0.055	0.425	0.059	0.132	0.060	0.041
25	0.787	0.114	0.896	0.116	0.034	0.748	0.074	0.517	0.071	0.032

Table 4: Empirical size of tests (i)–(v) ( $\rho = 0.5$ )

dim	n: 500					n: 1000				
	naive	bonfe	Wald	Max	sWald	naive	bonfe	Wald	Max	sWald
3	0.177	0.053	0.072	0.061	0.060	0.167	0.045	0.054	0.051	0.050
5	0.252	0.058	0.107	0.071	0.060	0.234	0.051	0.072	0.060	0.055
10	0.362	0.076	0.248	0.092	0.068	0.327	0.051	0.119	0.062	0.054
25	0.545	0.076	0.862	0.097	0.060	0.500	0.058	0.468	0.073	0.051

Table 5: Empirical size of tests (i)–(v) ( $\rho = 0.9$ )

dim	n: 500					n: 1000				
	naive	bonfe	Wald	Max	sWald	naive	bonfe	Wald	Max	sWald
3	0.132	0.042	0.066	0.055	0.060	0.124	0.033	0.051	0.049	0.053
5	0.150	0.036	0.090	0.059	0.048	0.149	0.035	0.068	0.054	0.050
10	0.186	0.037	0.216	0.072	0.070	0.169	0.023	0.104	0.050	0.050
25	0.226	0.024	0.820	0.060	0.056	0.204	0.018	0.406	0.047	0.047

*Notes:* (i) “naive”: empirical size of naive testing; (ii) “bonfe”: empirical size of Bonferroni correction; (iii) “Max”: empirical size of the Max test; (iv) “Wald”: empirical size of the Wald (chi-square) test; (v) “sWald”: standardized Wald (chi-square) test; “dim”: dimension of the pre-treatment covariates  $Z_i = (Z_{1,i}, \dots, Z_{d,i})'$ ; Columns under “n: 500” and “n: 1000” report the results obtained with size  $n = 500$  and  $n = 1000$ , respectively.

The performances of the other methods vary according to sample size, dimension

of covariates, and correlation coefficients. For the relatively small sample size of  $n = 500$ , the superiority of these methods is ambiguous. For a relatively small number of covariates  $dim \in \{1, 3, 5\}$ , the sWald test controls for size by 6%, whereas the Max test and Bonferroni correction control for size by approximately 7%. For a larger number of covariates, the Bonferroni correction and Max test may fail to control size by 10%, whereas the sWald test controls size by 7% throughout. For a larger sample size of  $n = 1000$ , the sWald test dominates the Bonferroni correction for size control. The sWald test controls size by 5.5% for any correlation and number of covariates up to 25.<sup>14</sup> For a moderate number of covariates up to  $dim = 5$  or 10, the Max test can control the size by 6% and is not substantially worse than the Bonferroni correction. Therefore, when the sample size is not small, the sWald test can control the size for any dimension up to  $dim = 25$ ; the Max test and Bonferroni correction can control the size up to  $dim = 5$  or 10.

Given the results of size control, we evaluate their empirical power properties. We compare the empirical power of the (ii) Bonferroni correction, (iv) Max test, and (v) sWald test under  $\bar{p} = 0.575$  and  $\tau_{Z_a}(= a) = 0, 0.5, 1, 1.5, 2$  for different dimensions  $d = 1, 3, 5$ . Figure 4 presents the results for the scalar covariate. Figures 5, and 6 present the results when one of the  $d$  covariates sees a jump. Further, Figures 7 and 8 show the results when all  $d$  covariates see a jump. However, each jump size is divided by  $d$  for  $d = 3, 5$ . In Figures 5–8, each figure presents the results for different correlations  $\rho = 0.5, 0.9$ .<sup>15</sup>

In all cases, the Max test exhibits higher power than the Bonferroni correction. When one of the covariates jumps (Figures 5 and 6), the Max test outperforms the Bonferroni correction and sWald test, and the gap among the three methods expands as the correlation and dimension increase. While the sWald test has relatively less power to detect small jumps in the covariate, the power of the sWald test catches up quickly as the jump size increases.

When all covariates have seen jumps (see Figure 7 and 8), the sWald test outperforms the Max test and Bonferroni correction in most cases. When the correlation is weak, the sWald test is substantially superior to the other two methods; however, the

---

<sup>14</sup>We consider that the failure in the Bonferroni correction comes from challenges in evaluating the tail of the nonparametric test statistics.

<sup>15</sup>In Appendix D, we present the results for weaker correlations and results containing negative correlations.

Max test approaches the sWald test as the correlation and dimensions increase. In Appendix D, we report qualitatively similar simulation results for other specifications, including lower or negative correlation coefficients.

To summarize, we recommend the Max test when one suspects that a few covariates exhibit jumps but not the others among a moderate number of covariates. We recommend the sWald test for other cases because it has superior size control and power properties for detecting jumps among many covariates.

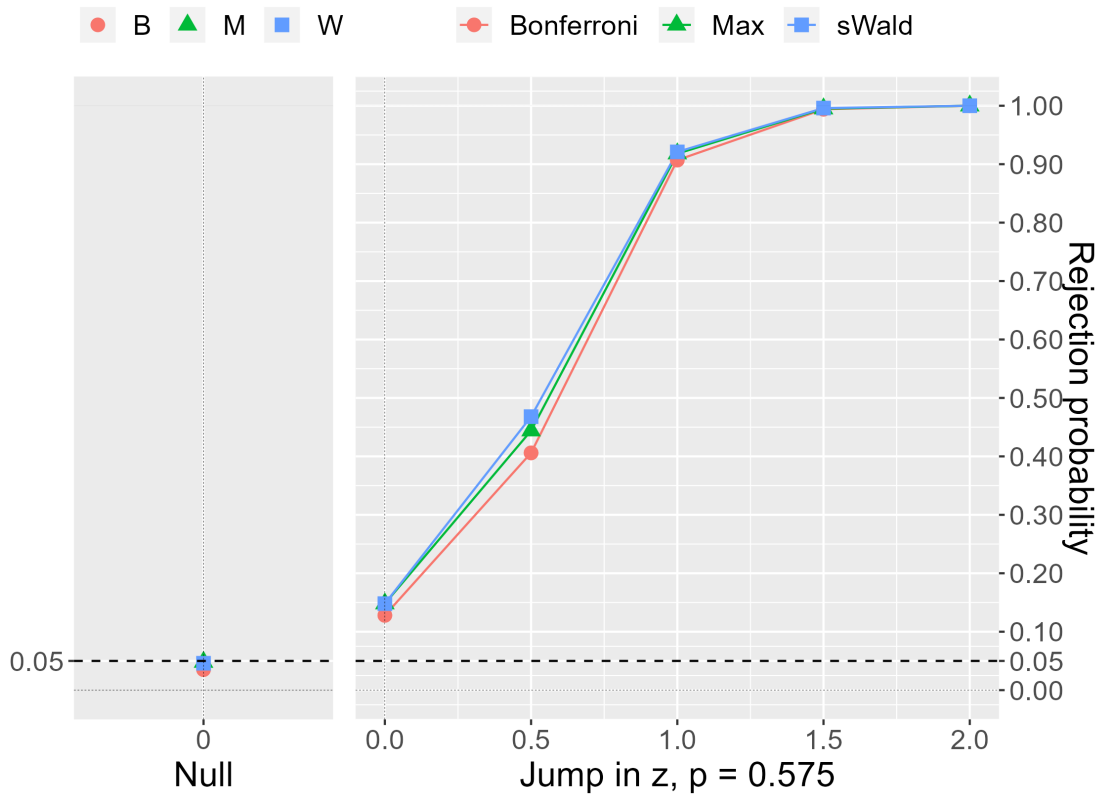
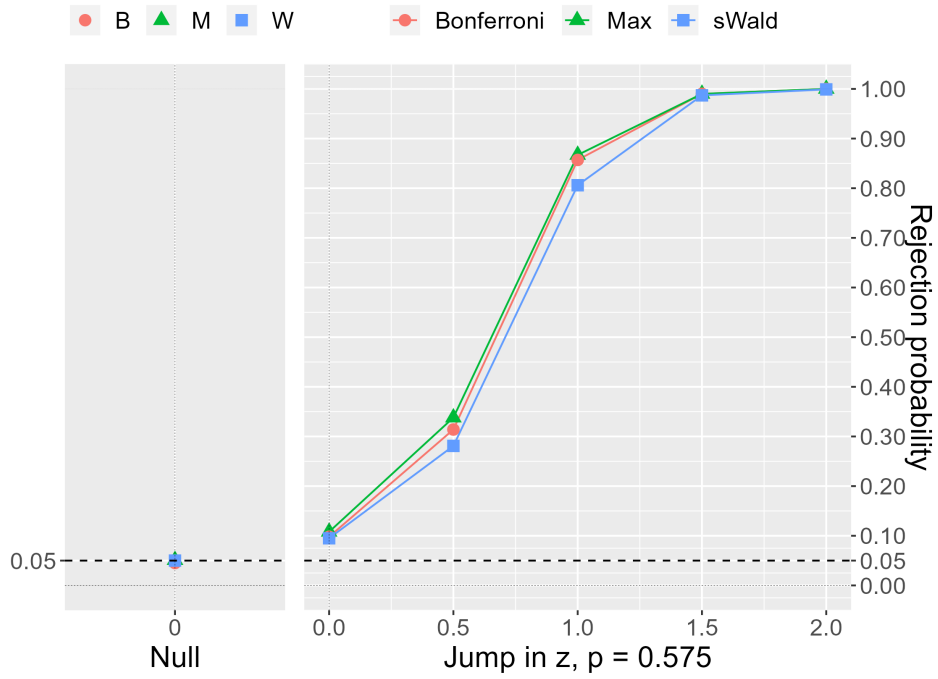
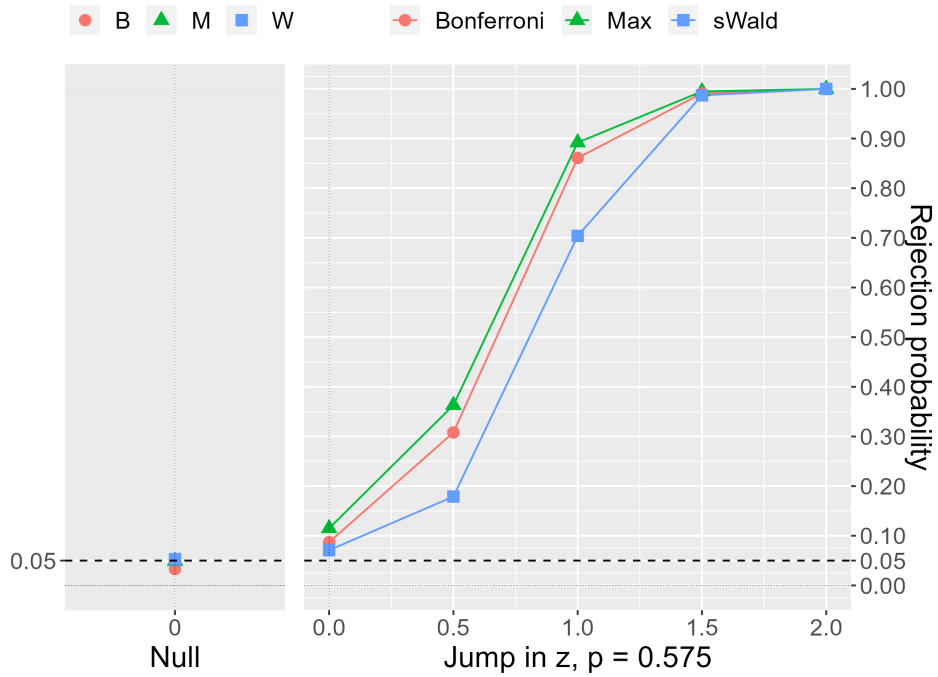


Figure 4: A jump in a scalar  $Z$  and a density test,  $n = 1000$

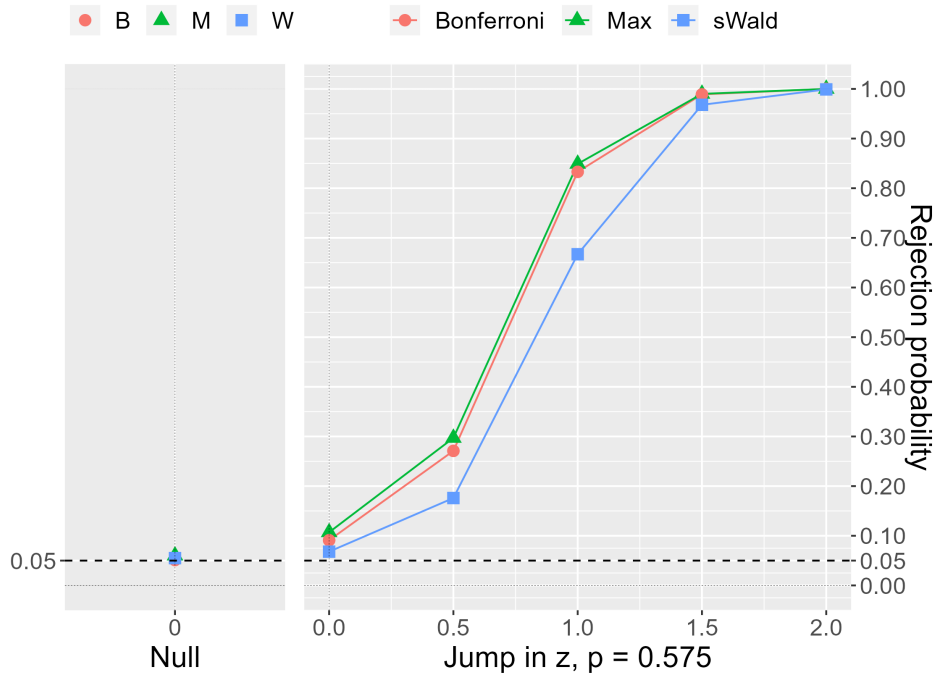


(a) Covariates have the same pairwise correlation coefficient of 0.5

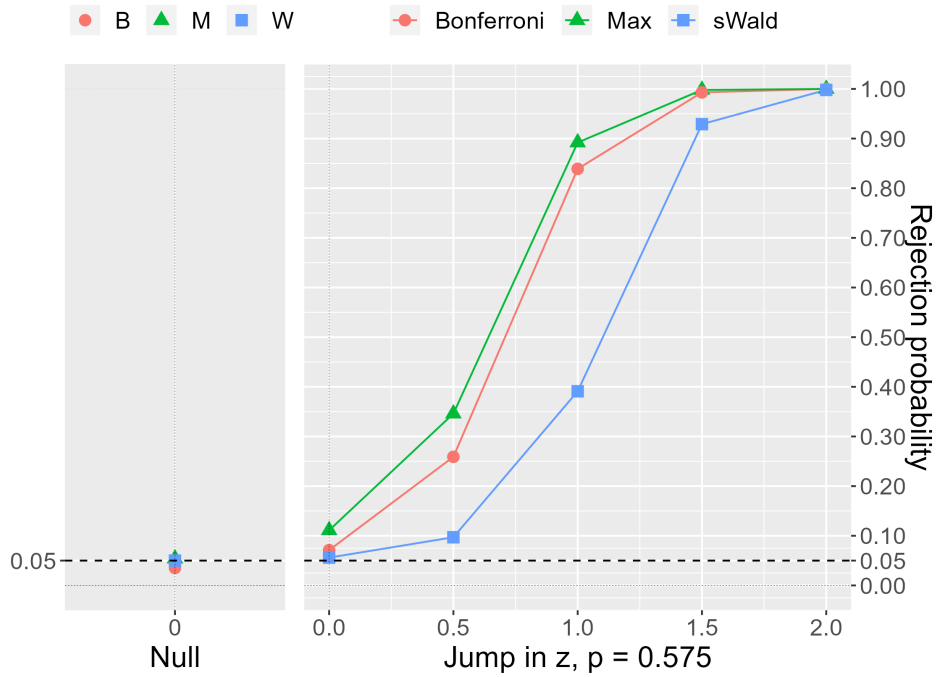


(b) Covariates have the same pairwise correlation coefficient of 0.9

Figure 5: A jump in the three covariates with a density,  $n = 1000$



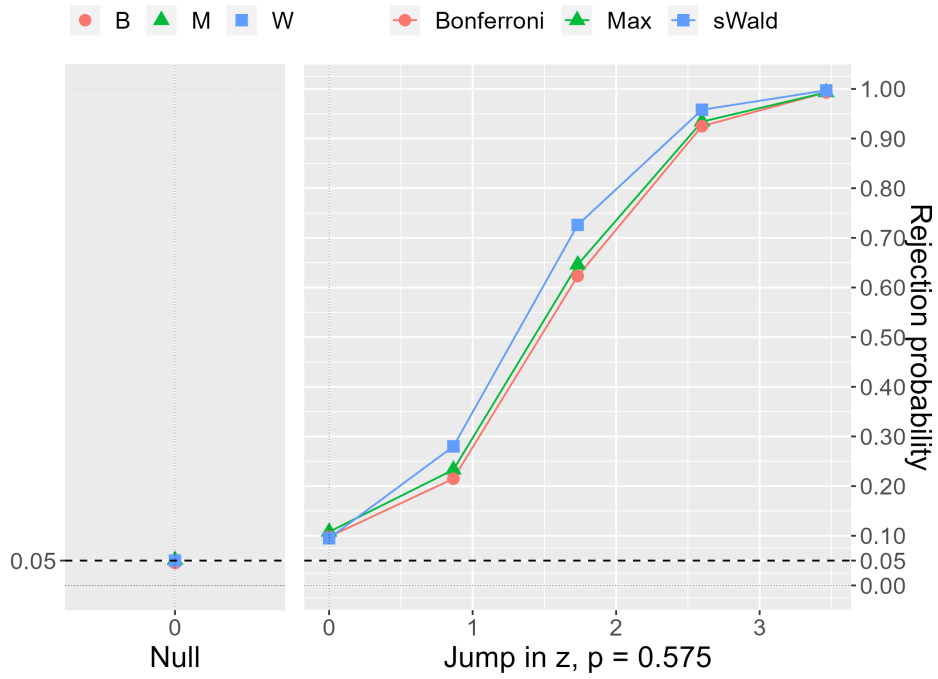
(a) Covariates have the same pairwise correlation coefficient of 0.5



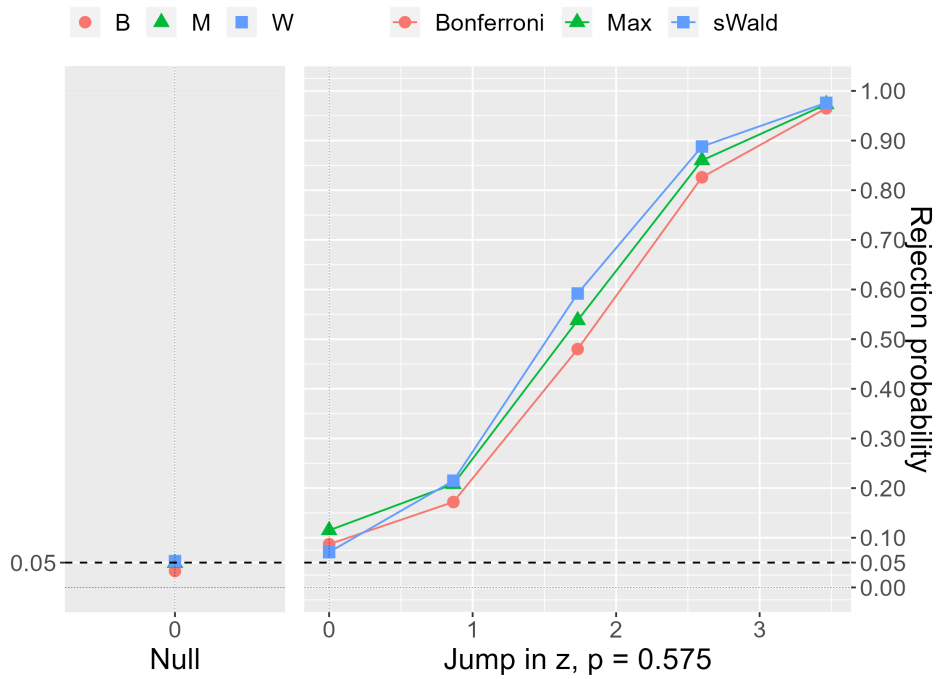
(b) Covariates have the same pairwise correlation coefficient of 0.9

Figure 6: A jump in the five covariates with a density,  $n = 1000$



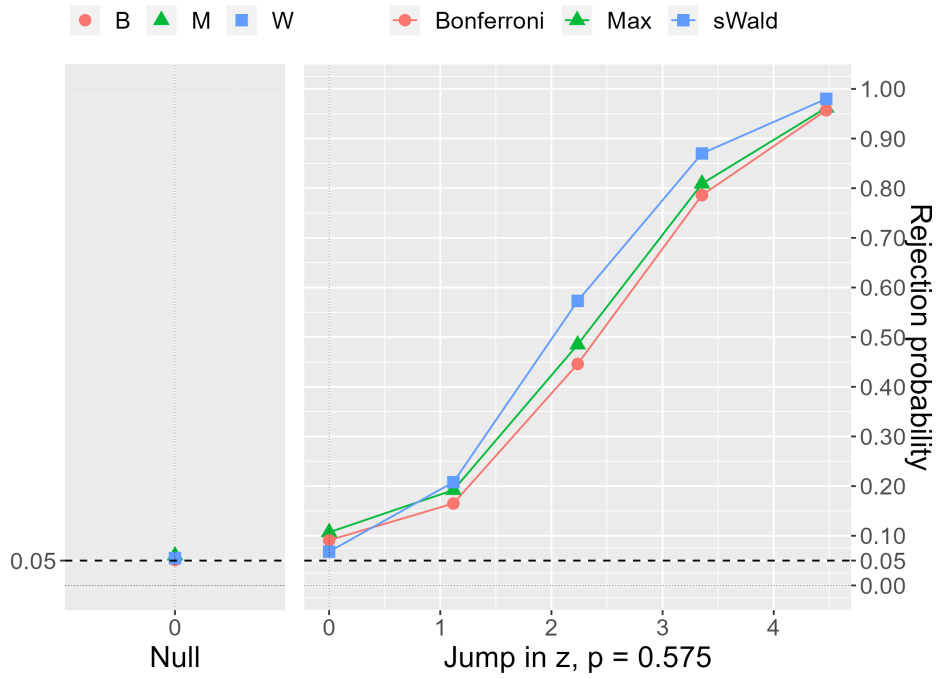


(a) Covariates have the same pairwise correlation coefficient of 0.5

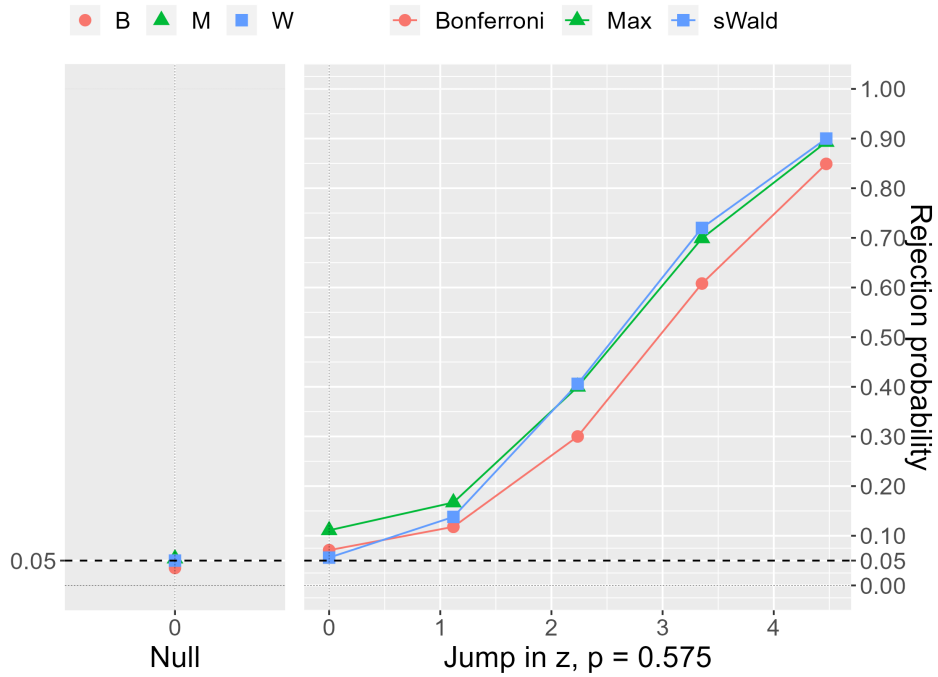


(b) Covariates have the same pairwise correlation coefficient of 0.9

Figure 7: 1/3 of jumps in all the three covariates with density,  $n = 1000$



(a) Covariates have the same pairwise correlation coefficient of 0.5



(b) Covariates have the same pairwise correlation coefficient of 0.9

Figure 8: 1/5 of jumps in all the five covariates with density,  $n = 1000$

## 5 Conclusion

Diagnostic tests are vital for applied studies of RD designs; however, their inappropriate use frustrates their purpose. The diagnostic procedure for RD design aims to test the underlying null hypothesis that all pre-determined covariates balance and the density function is continuous. Current practices test these restrictions separately without appropriate size control—they over-reject the null hypothesis that the identifying restriction for the RD design is valid.

We demonstrate an extraordinary over-rejection of the null hypothesis, where each testable restriction is valid. Among the 60 studies published in the top five economics journals, 35% (21 studies) rejected at least one testable restriction. Nevertheless, less than 5% of the 799 tests were rejected. Hence, we conclude that the underlying null hypothesis of local randomization is highly over-rejected where the underlying null hypotheses appear to hold. We blame the multiple testing problem for the over-rejection because most studies run more than 10 covariates balance tests separately.

We provide a solution to this over-rejection problem. We demonstrate the joint asymptotic normality of RD design estimators and provide alternative unified testing procedures. We show two different unified tests: the standardized Wald (sWald) test and the Max test. In the numerical simulations, the sWald and Max statistics achieved appropriate size-control properties for a moderate number of covariates when the sample size was 1000. The sWald test is particularly superior to other methods in size control, as it can control for any dimension of covariates up to 25 where the Bonferroni correction may fail to control the size. The power properties vary according to the underlying alternative hypotheses. The Max test is superior to the Bonferroni correction when only one covariate exhibits a jump in the conditional mean. The sWald test is superior to the Bonferroni correction when all the covariates jump in their conditional means.

In conclusion, we recommend the Max test for a design with a moderate number of covariates when only a few covariates violate local randomization. We recommend the sWald test for other designs. This test is appropriate for most practical designs where there is no ex-ante concern concerning covariate and testing many covariate balancing is the norm.

Based on our findings, we consider several topics for future research. First, finding another use for testable restrictions may be preferable. To validate local randomization,

we must focus on the underlying null hypothesis rather than detecting which restrictions fail. Nevertheless, if we detect a particular subgroup of covariates that invalidate local randomization, such a finding may provide valuable information. Diagnostic procedures using such information may improve design validation. Second, although we focused on the statistical inference of testable restrictions, a graphical analysis of testable restrictions is also important. Recent studies, such as Calonico, Cattaneo, and Titiunik (2015), have considered the optimal procedure for visualization, and Korting, Lieberman, Matsudaira, Pei, and Shen (2023) have demonstrated that tuning parameters in visualization is critical. We recommend our unified testing along with graphical analysis, with multiple testing problems in graphical analyses as a future research topic. Third, the diagnostic tests are essentially pre-testing before the ultimate testing for the treatment effect. We resolved this problem in diagnostic testing using a unified test for testable restrictions. Considering a joint test with an ultimate test for treatment effects is an important future question that involves conceptual and technical difficulties. Finally, evaluating the joint distribution of testing statistics that are nonparametric estimates is challenging. We will consider these issues as future research questions.

## A Formal results

Appendix A provides formal theoretical results and proofs.

### A.1 Setup and Notation

Let  $|\cdot|$  denote the Euclidean matrix norm, that is,  $|A|^2 = \text{trace}(A'A) = \sum_{j=1}^n \sum_{i=1}^m a_{ij}^2$  for  $(m \times n)$  matrix  $A = \{a_{ij}\}_{i=1, \dots, m}^{j=1, \dots, n}$ , and  $|a|^4 = |aa'|^2 = \sum_{j=1}^n \sum_{i=1}^n a_i^2 a_j^2$  for  $(n \times 1)$  vector  $a = (a_1, \dots, a_n)'$ . Let  $a_n \lesssim b_n$  denote  $a_n \leq Cb_n$  for a positive constant  $C$ , which is independent of  $n$ .

The estimands of the local polynomial estimators are

$$\beta_{Z_k+, l} = \left[ \mu_{Z_k+}, \frac{\mu_{Z_k+}^{(1)}}{1!}, \dots, \frac{\mu_{Z_k+}^{(l)}}{l!} \right]', \quad \beta_{Z_k-, l} = \left[ \mu_{Z_k-}, \frac{\mu_{Z_k-}^{(1)}}{1!}, \dots, \frac{\mu_{Z_k-}^{(l)}}{l!} \right]',$$

$$\beta_{f+, p} = \left[ F_+, \frac{f_+}{1!}, \frac{f_+^{(1)}}{2!}, \dots, \frac{f_+^{(p-1)}}{p!} \right]', \quad \beta_{f-, p} = \left[ F_-, \frac{f_-}{1!}, \frac{f_-^{(1)}}{2!}, \dots, \frac{f_-^{(p-1)}}{p!} \right]',$$

where  $F(x) = E[1\{X \leq x\}]$ ,  $F_+ = \lim_{x \rightarrow 0^+} F(x)$ ,  $F_- = \lim_{x \rightarrow 0^-} F(x)$ .

We set  $Z_k = (Z_{k,1}, \dots, Z_{k,n})'$ ,  $\tilde{F} = (\tilde{F}(X_1), \dots, \tilde{F}(X_n))'$ ,  $K_h(u) = K(u/h)/h$ ,  $H_p(h) = \text{diag}(1, h, \dots, h^p)$ ,  $X_p(h) = [r_p(X_1/h), \dots, r_p(X_n/h)]'$ ,

$$W_+(h) = \text{diag}(1\{X_1 \geq 0\}K_h(X_1), \dots, 1\{X_n \geq 0\}K_h(X_n)),$$

$$W_-(h) = \text{diag}(1\{X_1 < 0\}K_h(X_1), \dots, 1\{X_n < 0\}K_h(X_n)),$$

$$\Gamma_{+,p}(h) = \frac{1}{n}X_p(h)'W_+(h)X_p(h), \quad \Gamma_{-,p}(h) = \frac{1}{n}X_p(h)'W_-(h)X_p(h),$$

The local polynomial estimators are as follows.

$$\hat{\beta}_{Z_{k+,l}}(h_k) = \frac{1}{n}H_l^{-1}(h_k)\Gamma_{+,l}^{-1}(h_k)X_l(h_k)'W_+(h_k)Z_k,$$

$$\hat{\beta}_{Z_{k-,l}}(h_k) = \frac{1}{n}H_l^{-1}(h_k)\Gamma_{-,l}^{-1}(h_k)X_l(h_k)'W_-(h_k)Z_k,$$

and

$$\hat{\beta}_{f_{+,p}}(h_f) = \frac{1}{n}H_p^{-1}(h_f)\Gamma_{+,p}^{-1}(h_f)X_p(h_f)'W_+(h_f)\tilde{F},$$

$$\hat{\beta}_{f_{-,p}}(h_f) = \frac{1}{n}H_p^{-1}(h_f)\Gamma_{-,p}^{-1}(h_f)X_p(h_f)'W_-(h_f)\tilde{F}.$$

Let

$$\Delta\hat{\mu}_{Z_{k+,l}}(h_k) \equiv \sqrt{nh_k}[\hat{\mu}_{Z_{k+,l}}(h_k) - \mu_{Z_{k+}}], \quad \Delta\hat{\mu}_{Z_{k-,l}}(h_k) \equiv \sqrt{nh_k}[\hat{\mu}_{Z_{k-,l}}(h_k) - \mu_{Z_{k-}}],$$

$$\Delta\hat{f}_{+,p}(h_f) \equiv \sqrt{nh_f}[\hat{f}_{+,p}(h_f) - f_+], \quad \Delta\hat{f}_{-,p}(h_f) \equiv \sqrt{nh_f}[\hat{f}_{-,p}(h_f) - f_-].$$

Letting  $\mathcal{X}_n = (X_1, \dots, X_n)'$ , we decompose  $\Delta\hat{\mu}_{Z_{k+,l}}(h_k)$  and  $\Delta\hat{\mu}_{Z_{k-,l}}(h_k)$  as

$$\Delta\hat{\mu}_{Z_{k+,l}}(h_k) = \Delta^M\hat{\mu}_{Z_{k+,l}}(h_k) + \Delta^B\hat{\mu}_{Z_{k+,l}}(h_k),$$

$$\Delta\hat{\mu}_{Z_{k-,l}}(h_k) = \Delta^M\hat{\mu}_{Z_{k-,l}}(h_k) + \Delta^B\hat{\mu}_{Z_{k-,l}}(h_k),$$

where

$$\Delta^M\hat{\mu}_{Z_{k+,l}}(h_k) \equiv \sqrt{nh_k}\{\hat{\mu}_{Z_{k+,l}}(h_k) - E[\hat{\mu}_{Z_{k+,l}}(h_k)|\mathcal{X}_n]\},$$

$$\Delta^M\hat{\mu}_{Z_{k-,l}}(h_k) \equiv \sqrt{nh_k}\{\hat{\mu}_{Z_{k-,l}}(h_k) - E[\hat{\mu}_{Z_{k-,l}}(h_k)|\mathcal{X}_n]\}$$

and

$$\Delta^B\hat{\mu}_{Z_{k+,l}}(h_k) \equiv \sqrt{nh_k}\{E[\hat{\mu}_{Z_{k+,l}}(h_k)|\mathcal{X}_n] - \mu_{Z_{k+}}\},$$

$$\Delta^B\hat{\mu}_{Z_{k-,l}}(h_k) \equiv \sqrt{nh_k}\{E[\hat{\mu}_{Z_{k-,l}}(h_k)|\mathcal{X}_n] - \mu_{Z_{k-}}\}.$$

$\Delta^B\hat{\mu}_{Z_{k+,l}}(h_k)$  and  $\Delta^B\hat{\mu}_{Z_{k-,l}}(h_k)$  represent the smoothing bias. We consider the distributional approximations of  $\Delta^M\hat{\mu}_{Z_{k+,l}}(h_k)$  and  $\Delta^M\hat{\mu}_{Z_{k-,l}}(h_k)$ .

We define  $\tilde{f}_{+,p}(h_f)$  and  $\tilde{f}_{-,p}(h_f)$  as slope coefficients in the following local polynomial regressions.

$$\tilde{f}_{+,p}(h_f) = e'_1 \tilde{\beta}_{f+,p}(h_f), \quad \tilde{f}_{-,p}(h_f) = e'_1 \tilde{\beta}_{f-,p}(h_f),$$

where

$$\begin{aligned} \tilde{\beta}_{f+,p}(h_f) &= \arg \min_{\beta \in \mathbb{R}^{p+1}} \sum_{i=1}^n 1\{X_i \geq 0\} (F(X_i) - r_p(X_i)' \beta)^2 K_{h_f}(X_i), \\ \tilde{\beta}_{f-,p}(h_f) &= \arg \min_{\beta \in \mathbb{R}^{p+1}} \sum_{i=1}^n 1\{X_i < 0\} (F(X_i) - r_p(X_i)' \beta)^2 K_{h_f}(X_i). \end{aligned}$$

$\tilde{f}_{+,p}(h_f)$  and  $\tilde{f}_{-,p}(h_f)$  are obtained from  $p$ th-order local polynomial one-sided approximations of the true distribution of  $X_i$ . We decompose  $\Delta \hat{f}_{+,p}(h_f)$  and  $\Delta \hat{f}_{-,p}(h_f)$  as

$$\Delta \hat{f}_{+,p}(h_f) = \Delta^{M_0} \hat{f}_{+,p}(h_f) + \Delta^{B_0} \hat{f}_{+,p}(h_f), \quad \Delta \hat{f}_{-,p}(h_f) = \Delta^{M_0} \hat{f}_{-,p}(h_f) + \Delta^{B_0} \hat{f}_{-,p}(h_f),$$

where

$$\begin{aligned} \Delta^{M_0} \hat{f}_{+,p}(h_f) &\equiv \sqrt{nh_f} \{ \hat{f}_{+,p}(h_f) - \tilde{f}_{+,p}(h_f) \}, \\ \Delta^{M_0} \hat{f}_{-,p}(h_f) &\equiv \sqrt{nh_f} \{ \hat{f}_{-,p}(h_f) - \tilde{f}_{-,p}(h_f) \} \end{aligned}$$

and

$$\Delta^{B_0} \hat{f}_{+,p}(h_f) \equiv \sqrt{nh_f} \{ \tilde{f}_{+,p}(h_f) - f_+ \}, \quad \Delta^{B_0} \hat{f}_{-,p}(h_f) \equiv \sqrt{nh_f} \{ \tilde{f}_{-,p}(h_f) - f_- \}.$$

$\Delta^{B_0} \hat{f}_{+,p}(h_f)$  and  $\Delta^{B_0} \hat{f}_{-,p}(h_f)$  represent smoothing bias. We set  $F = (F(X_1), \dots, F(X_n))'$ ,  $\iota = (1, \dots, 1)'$ , which are  $n$ -dimensional.

$$\begin{aligned} U_{+,p}(h_f) &\equiv \frac{1}{n(n-1)} \sum_{i,j:i \neq j}^n \psi_{+,p,h_f}(X_i, X_j), \\ U_{-,p}(h_f) &\equiv \frac{1}{n(n-1)} \sum_{i,j:i \neq j}^n \psi_{-,p,h_f}(X_i, X_j), \end{aligned}$$

where

$$\begin{aligned} \psi_{+,p,h_f}(X_i, X_j) &\equiv 1\{X_i \geq 0\} r_p(X_i/h_f) (1\{X_j \leq X_i\} - F(X_i)) K_{h_f}(X_i), \\ \psi_{-,p,h_f}(X_i, X_j) &\equiv 1\{X_i < 0\} r_p(X_i/h_f) (1\{X_j \leq X_i\} - F(X_i)) K_{h_f}(X_i). \end{aligned}$$

We further decompose  $\Delta^{M_0} \hat{f}_{+,p}(h_f)$  and  $\Delta^{M_0} \hat{f}_{-,p}(h_f)$  as follows.

$$\begin{aligned}\Delta^{M_0} \hat{f}_{+,p}(h_f) &= \Delta^{M_1} \hat{f}_{+,p}(h_f) + \Delta^{B_1} \hat{f}_{+,p}(h_f), \\ \Delta^{M_0} \hat{f}_{-,p}(h_f) &= \Delta^{M_1} \hat{f}_{-,p}(h_f) + \Delta^{B_1} \hat{f}_{-,p}(h_f),\end{aligned}$$

where

$$\begin{aligned}\Delta^{M_1} \hat{f}_{+,p}(h_f) &\equiv \left(1 - \frac{1}{n}\right) \sqrt{\frac{n}{h_f}} e_1' \Gamma_{+,p}^{-1}(h_f) U_{+,p}(h_f), \\ \Delta^{M_1} \hat{f}_{-,p}(h_f) &\equiv \left(1 - \frac{1}{n}\right) \sqrt{\frac{n}{h_f}} e_1' \Gamma_{-,p}^{-1}(h_f) U_{-,p}(h_f),\end{aligned}$$

and

$$\begin{aligned}\Delta^{B_1} \hat{f}_{+,p}(h_f) &\equiv \frac{1}{\sqrt{nh_f}} \frac{1}{n} e_1' \Gamma_{+,p}^{-1}(h_f) X_p(h_f)' W_+(h_f) (\iota - F), \\ \Delta^{B_1} \hat{f}_{-,p}(h_f) &\equiv \frac{1}{\sqrt{nh_f}} \frac{1}{n} e_1' \Gamma_{-,p}^{-1}(h_f) X_p(h_f)' W_-(h_f) (\iota - F).\end{aligned}$$

$U_{+,p}(h_f)$  and  $U_{-,p}(h_f)$  are considered second-order U-statistics (where the kernels  $\psi_{+,p,h_f}(X_i, X_j)$  and  $\psi_{-,p,h_f}(X_i, X_j)$  are  $(p+1)$ -dimensional and depend on the bandwidth  $h_f$ ), and  $\Delta^{B_1} \hat{f}_{+,p}(h_f)$  and  $\Delta^{B_1} \hat{f}_{-,p}(h_f)$  represent the leave-in bias. These terms arise because the empirical distribution function  $\tilde{F}(X_i)$  is approximated, which leads to double summation. Note that  $E[\psi_{+,p,h_f}(X_i, X_j)] = 0$  and  $E[\psi_{-,p,h_f}(X_i, X_j)] = 0$ . U-statistics can be decomposed as

$$U_{+,p}(h_f) = U_{1,+,p}(h_f) + U_{2,+,p}(h_f), \quad U_{-,p}(h_f) = U_{1,-,p}(h_f) + U_{2,-,p}(h_f)$$

with

$$U_{1,+,p}(h_f) \equiv \frac{1}{n} \sum_{i=1}^n E[\psi_{+,p,h_f}(X_j, X_i) | X_i], \quad U_{1,-,p}(h_f) \equiv \frac{1}{n} \sum_{i=1}^n E[\psi_{-,p,h_f}(X_j, X_i) | X_i]$$

for  $j \neq i$  and

$$\begin{aligned}U_{2,+,p}(h_f) &\equiv \frac{1}{n(n-1)} \sum_{i,j:i \neq j}^n \varphi_{+,p,h_f}(X_i, X_j), \\ U_{2,-,p}(h_f) &\equiv \frac{1}{n(n-1)} \sum_{i,j:i \neq j}^n \varphi_{-,p,h_f}(X_i, X_j),\end{aligned}$$

where

$$\begin{aligned}\varphi_{+,p,h_f}(X_i, X_j) &\equiv \psi_{+,p,h_f}(X_i, X_j) + \psi_{+,p,h_f}(X_j, X_i) \\ &\quad - E[\psi_{+,p,h_f}(X_i, X_j) | X_j] - E[\psi_{+,p,h_f}(X_j, X_i) | X_i],\end{aligned}$$

$$\begin{aligned}\varphi_{-,p,h_f}(X_i, X_j) &\equiv \psi_{-,p,h_f}(X_i, X_j) + \psi_{-,p,h_f}(X_j, X_i) \\ &\quad - E[\psi_{-,p,h_f}(X_i, X_j)|X_j] - E[\psi_{-,p,h_f}(X_j, X_i)|X_i].\end{aligned}$$

This decomposition is often referred to as the Hoeffding decomposition (see, e.g., Serfling (1980)).  $U_{2,+p}(h_f)$  and  $U_{2,-p}(h_f)$  are degenerate U-statistics that are later shown to be asymptotically negligible under our assumptions. Let

$$\begin{aligned}\Delta^{B_2} \hat{f}_{+,p}(h_f) &\equiv \sqrt{\frac{n}{h_f}} e'_1 \Gamma_{+,p}^{-1}(h_f) U_{2,+p}(h_f), \\ \Delta^{B_2} \hat{f}_{-,p}(h_f) &\equiv \sqrt{\frac{n}{h_f}} e'_1 \Gamma_{-,p}^{-1}(h_f) U_{2,-p}(h_f), \\ \Delta^{B_3} \hat{f}_{+,p}(h_f) &\equiv -\frac{1}{\sqrt{nh_f}} e'_1 \Gamma_{+,p}^{-1}(h_f) U_{+,p}(h_f), \\ \Delta^{B_3} \hat{f}_{-,p}(h_f) &\equiv -\frac{1}{\sqrt{nh_f}} e'_1 \Gamma_{-,p}^{-1}(h_f) U_{-,p}(h_f).\end{aligned}$$

We can decompose  $\Delta \hat{f}_{+,p}(h_f)$  and  $\Delta \hat{f}_{-,p}(h_f)$  into

$$\Delta \hat{f}_{+,p}(h_f) = \Delta^M \hat{f}_{+,p}(h_f) + \Delta^B \hat{f}_{+,p}(h_f), \quad \Delta \hat{f}_{-,p}(h_f) = \Delta^M \hat{f}_{-,p}(h_f) + \Delta^B \hat{f}_{-,p}(h_f),$$

where

$$\Delta^M \hat{f}_{+,p}(h_f) \equiv \sqrt{\frac{n}{h_f}} e'_1 \Gamma_{+,p}^{-1}(h_f) U_{1,+p}(h_f), \quad \Delta^M \hat{f}_{-,p}(h_f) \equiv \sqrt{\frac{n}{h_f}} e'_1 \Gamma_{-,p}^{-1}(h_f) U_{1,-p}(h_f)$$

and

$$\Delta^B \hat{f}_{+,p}(h_f) \equiv \sum_{j=0}^3 \Delta^{B_j} \hat{f}_{+,p}(h_f), \quad \Delta^B \hat{f}_{-,p}(h_f) \equiv \sum_{j=0}^3 \Delta^{B_j} \hat{f}_{-,p}(h_f).$$

We consider distributional approximations of  $\Delta^M \hat{f}_{+,p}(h_f)$  and  $\Delta^M \hat{f}_{-,p}(h_f)$ .

To characterize the bias and variance of the local polynomial estimators, we employ the following notation.

$$\begin{aligned}\sigma_{Z_k+}^2 &= \lim_{x \rightarrow 0^+} \sigma_{Z_k}^2(x), \quad \sigma_{Z_k-}^2 = \lim_{x \rightarrow 0^-} \sigma_{Z_k}^2(x), \quad \sigma_{Z_k}^2(x) = \text{Var}(Z_k | X = x), \\ \sigma_{Z_j Z_k+} &= \lim_{x \rightarrow 0^+} \sigma_{Z_j Z_k}(x), \quad \sigma_{Z_j Z_k-} = \lim_{x \rightarrow 0^-} \sigma_{Z_j Z_k}(x), \quad \sigma_{Z_j Z_k}(x) = \text{Cov}(Z_j, Z_k | X = x), \\ \varepsilon_{Z_k} &= (\varepsilon_{Z_k,1}, \dots, \varepsilon_{Z_k,n})' \text{ with } \varepsilon_{Z_k,i} = Z_{k,i} - \mu_{Z_k}(X_i), \\ \Sigma_{Z_k} &= E[\varepsilon_{Z_k} \varepsilon'_{Z_k} | \mathcal{X}_n] = \text{diag}(\sigma_{Z_k}^2(X_1), \dots, \sigma_{Z_k}^2(X_n)), \\ \Sigma_{Z_j Z_k} &= E[\varepsilon_{Z_j} \varepsilon'_{Z_k} | \mathcal{X}_n] = \text{diag}(\sigma_{Z_j Z_k}(X_1), \dots, \sigma_{Z_j Z_k}(X_n)),\end{aligned}$$



$$\begin{aligned}
S_p(h) &= [(X_1/h)^p, \dots, (X_n/h)^p]', \\
\vartheta_{+,p,q}(h) &= X_p(h)'W_+(h)S_q(h)/n, \quad \vartheta_{-,p,q}(h) = X_p(h)'W_-(h)S_q(h)/n, \\
\Psi_{Z_j Z_{k+},p,q}(h_j, h_k) &= X_p(h_j)'W_+(h_j)\Sigma_{Z_j Z_k} W_+(h_k)X_q(h_k)/n, \\
\Psi_{Z_j Z_{k-},p,q}(h_j, h_k) &= X_p(h_j)'W_-(h_j)\Sigma_{Z_j Z_k} W_-(h_k)X_q(h_k)/n, \\
\Psi_{Z_{k+},p}(h) &= \Psi_{Z_k Z_{k+},p,p}(h, h) = X_p(h)'W_+(h)\Sigma_{Z_k} W_+(h)X_p(h)/n, \\
\Psi_{Z_{k-},p}(h) &= \Psi_{Z_k Z_{k-},p,p}(h, h) = X_p(h)'W_-(h)\Sigma_{Z_k} W_-(h)X_p(h)/n, \\
\tilde{\Psi}_{Z_j Z_{k+},p,q}(h_j, h_k) &= \int_0^\infty K\left(\frac{h_{jk}u}{h_j}\right) K\left(\frac{h_{jk}u}{h_k}\right) r_p\left(\frac{h_{jk}u}{h_j}\right) r_q\left(\frac{h_{jk}u}{h_k}\right)' \sigma_{Z_j Z_k}^2(uh_{jk})f(uh_{jk})du, \\
\tilde{\Psi}_{Z_j Z_{k-},p,q}(h_j, h_k) &= \int_0^\infty K\left(\frac{h_{jk}u}{h_j}\right) K\left(\frac{h_{jk}u}{h_k}\right) r_p\left(\frac{h_{jk}u}{h_j}\right) r_q\left(\frac{h_{jk}u}{h_k}\right)' \sigma_{Z_j Z_k}^2(-uh_{jk})f(-uh_{jk})du, \\
\tilde{\Psi}_{Z_{k+},p}(h) &= \tilde{\Psi}_{Z_k Z_{k+},p,p}(h, h) = \int_0^\infty K(u)^2 r_p(u) r_p(u)' \sigma_{Z_k}^2(uh) f(uh) du, \\
\tilde{\Psi}_{Z_{k-},p}(h) &= \tilde{\Psi}_{Z_k Z_{k-},p,p}(h, h) = \int_0^\infty K(u)^2 r_p(u) r_p(u)' \sigma_{Z_k}^2(-uh) f(-uh) du, \\
\Gamma_p &= \int_0^\infty K(u) r_p(u) r_p(u)' du, \quad \vartheta_{p,q} = \int_0^\infty K(u) u^q r_p(u) du,
\end{aligned}$$

where  $h_{jk} = (h_j h_k)^{1/2}$ ,

$$\begin{aligned}
&\Psi_{jk,p,q} \\
&= \begin{cases} \int_0^\infty K((c_{jk})^{1/2}u) K((c_{jk})^{-1/2}u) r_p((c_{jk})^{1/2}u) r_q((c_{jk})^{-1/2}u)' du & \text{if } \rho_{jk} \rightarrow c_{jk} \\ 0 & \text{otherwise} \end{cases} \\
&= \begin{cases} (c_{jk})^{1/2} \int_0^\infty K(c_{jk}u) K(u) r_p(c_{jk}u) r_q(u)' du & \text{if } \rho_{jk} \rightarrow c_{jk} \\ 0 & \text{otherwise,} \end{cases}
\end{aligned}$$

for  $c_{jk} \in (0, \infty)$ ,

$$\begin{aligned}
\Psi_{p,q} &= \Psi_{kk,p,q} = \int_0^\infty K(u)^2 r_p(u) r_q(u)' du, \\
\Psi_{f,p} &= \int_0^\infty \int_0^\infty (u \wedge v) r_p(u) r_p(v)' K(u) K(v) dudv.
\end{aligned}$$

## A.2 Preliminary lemmas

First, we present the asymptotic bias, variance, and distribution of the local polynomial estimators. We provide the proofs of the lemmas in Appendix A.5.

The following lemma describes the asymptotic behavior of the bias terms for the local polynomial estimators.

**Lemma A.1.** *Suppose Assumptions 1-2 hold with  $S \geq l + 2$  and  $R \geq p + 1$ .*

(a) *If  $nh_{\min} \rightarrow \infty$  and  $h_{\max} \rightarrow 0$ , then*

$$\begin{aligned} & \Delta^B \hat{\mu}_{Z_k+,l}(h_k) \\ &= \sqrt{n}(h_k)^{3/2+l} B_{Z_k+,l,l+1}(h_k) + \sqrt{n}(h_k)^{5/2+l} B_{Z_k+,l,l+2}(h_k)[1 + o_p(1)], \end{aligned} \quad (\text{A.1})$$

$$\begin{aligned} & \Delta^B \hat{\mu}_{Z_k-,l}(h_k) \\ &= \sqrt{n}(h_k)^{3/2+l} B_{Z_k-,l,l+1}(h_k) + \sqrt{n}(h_k)^{5/2+l} B_{Z_k-,l,l+2}(h_k)[1 + o_p(1)], \end{aligned} \quad (\text{A.2})$$

where

$$B_{Z_k+,l,r}(h_k) = \frac{\mu_{Z_k+}^{(r)}}{r!} \mathcal{B}_{+,0,l,r}(h_k), \quad B_{Z_k-,l,r}(h_k) = \frac{\mu_{Z_k-}^{(r)}}{r!} \mathcal{B}_{-,0,l,r}(h_k), \quad (\text{A.3})$$

$$\mathcal{B}_{+,s,l,r}(h_k) = s! e'_s \Gamma_{+,l}^{-1}(h_k) \vartheta_{+,l,r}(h_k) = s! e'_s \Gamma_l^{-1} \vartheta_{l,r} + o_p(1), \quad (\text{A.4})$$

$$\mathcal{B}_{-,s,l,r}(h_k) = s! e'_s \Gamma_{-,l}^{-1}(h_k) \vartheta_{-,l,r}(h_k) = (-1)^{s+r} s! e'_s \Gamma_l^{-1} \vartheta_{l,r} + o_p(1). \quad (\text{A.5})$$

(b) *If  $nh_f \rightarrow \infty$  and  $h_f \rightarrow 0$ , then*

$$\begin{aligned} & \Delta^{B_0} \hat{f}_{+,p}(h_f) \\ &= \sqrt{n} h_f^{p+1/2} B_{f,+,p,p+1}(h_f) + \sqrt{n} h_f^{p+3/2} B_{f,+,p,p+2}(h_f)[1 + o_p(1)], \end{aligned} \quad (\text{A.6})$$

$$\Delta^{B_1} \hat{f}_{+,p}(h_f) = O_p((nh_f)^{-1/2}) = o_p(1),$$

$$\begin{aligned} & \Delta^{B_0} \hat{f}_{-,p}(h_f) \\ &= \sqrt{n} h_f^{p+1/2} B_{f,-,p,p+1}(h_f) + \sqrt{n} h_f^{p+3/2} B_{f,-,p,p+2}(h_f)[1 + o_p(1)], \end{aligned} \quad (\text{A.7})$$

$$\Delta^{B_1} \hat{f}_{-,p}(h_f) = o_p(1),$$

where

$$B_{f,+,p,q}(h_f) = \frac{f_+^{(q-1)}}{(q-1)!} \mathcal{B}_{+,1,p,q}(h_f), \quad B_{f,-,p,q}(h_f) = \frac{f_-^{(q-1)}}{(q-1)!} \mathcal{B}_{-,1,p,q}(h_f). \quad (\text{A.8})$$

(c) *If  $nh_f^2 \rightarrow \infty$  and  $h_f \rightarrow 0$ , then*

$$\Delta^{B_2} \hat{f}_{+,p}(h_f) = O_p((nh_f^2)^{-1/2}) = o_p(1), \quad \Delta^{B_2} \hat{f}_{-,p}(h_f) = o_p(1). \quad (\text{A.9})$$

Observe that

$$\Delta^M \hat{\mu}_{Z_k+,l}(h_k) = \sqrt{\frac{h_k}{n}} e_0' \Gamma_{+,l}^{-1}(h_k) X_l(h_k)' W_+(h_k) \varepsilon_{Z_k},$$

$$\Delta^M \hat{\mu}_{Z_k-,l}(h_k) = \sqrt{\frac{h_k}{n}} e_0' \Gamma_{-,l}^{-1}(h_k) X_l(h_k)' W_-(h_k) \varepsilon_{Z_k}.$$

The following lemma is used to derive the asymptotic variance of the local polynomial estimators.

**Lemma A.2.** *Suppose Assumptions 1-2 hold with  $S \geq l+2$  and  $R \geq p+1$ .*

(a) *If  $nh_{\min} \rightarrow \infty$  and  $h_{\max} \rightarrow 0$ , then*

$$\begin{aligned} & \text{Cov} \left( \sqrt{\frac{h_j}{n}} X_l(h_j)' W_+(h_j) \varepsilon_{Z_j}, \sqrt{\frac{h_k}{n}} X_l(h_k)' W_+(h_k) \varepsilon_{Z_k} \right) \\ &= f_+ \sigma_{Z_j Z_k+} \Psi_{jk,l,l} + o(1) \end{aligned}$$

and

$$\begin{aligned} & \text{Cov} \left( \sqrt{\frac{h_j}{n}} X_l(h_j)' W_-(h_j) \varepsilon_{Z_j}, \sqrt{\frac{h_k}{n}} X_l(h_k)' W_-(h_k) \varepsilon_{Z_k} \right) \\ &= f_- \sigma_{Z_j Z_k-} H_l(-1) \Psi_{jk,l,l} H_l(-1) + o(1). \end{aligned}$$

(b) *If  $nh_f^2 \rightarrow \infty$  and  $h_f \rightarrow 0$ , then*

$$\begin{aligned} & \text{Var} \left( \sqrt{\frac{n}{h_f}} U_{1,+,p}(h_f) \right) \\ &= \frac{1}{h_f} f_+^2 (F_+ - F_+^2) \Gamma_p e_0 e_0' \Gamma_p + f_+^3 \Psi_{f,p} \\ & \quad + \{ -f_+^3 F_+ + f_+ f_+' (F_+ - F_+^2) \} \Gamma_p (e_1 e_0' + e_0 e_1') \Gamma_p + o(1) \end{aligned}$$

and

$$\begin{aligned} & \text{Var} \left( \sqrt{\frac{n}{h_f}} U_{1,-,p}(h_f) \right) \\ &= \frac{1}{h_f} f_-^2 (F_- - F_-^2) H_p(-1) \Gamma_p e_0 e_0' \Gamma_p H_p(-1) + f_-^3 H_p(-1) \Psi_{f,p} H_p(-1) \\ & \quad - \{ -f_-^3 (F_- - 1) + f_- f_-' (F_- - F_-^2) \} H_p(-1) \Gamma_p (e_1 e_0' + e_0 e_1') \Gamma_p H_p(-1) \\ & \quad + o(1). \end{aligned}$$

(c)

$$\text{Cov} (X_l(h_k)' W_+(h_k) \varepsilon_{Z_k}, U_{1,+,p}(h_f)) = 0$$

and

$$\text{Cov}(X_l(h_k)'W_-(h_k)\varepsilon_{Z_k}, U_{1,-,p}(h_f)) = 0.$$

We set

$$\begin{aligned} C_{Z_j Z_{k+},l} &= \frac{\sigma_{Z_j Z_{k+}}^2}{f_+} e_0' \Gamma_l^{-1} \Psi_{jk,l,l} \Gamma_l^{-1} e_0, & C_{Z_j Z_{k-},l} &= \frac{\sigma_{Z_j Z_{k-}}^2}{f_-} e_0' \Gamma_l^{-1} \Psi_{jk,l,l} \Gamma_l^{-1} e_0, \\ V_{Z_{k+},l} = C_{Z_k Z_{k+},l} &= \frac{\sigma_{Z_k^+}^2}{f_+} e_0' \Gamma_l^{-1} \Psi_l \Gamma_l^{-1} e_0, & V_{Z_{k-},l} = C_{Z_k Z_{k-},l} &= \frac{\sigma_{Z_k^-}^2}{f_-} e_0' \Gamma_l^{-1} \Psi_l \Gamma_l^{-1} e_0, \\ V_{f,+ ,p} &= f_+ e_1' \Gamma_p^{-1} \Psi_{f,p} \Gamma_p^{-1} e_1, & V_{f,- ,p} &= f_- e_1' \Gamma_p^{-1} \Psi_{f,p} \Gamma_p^{-1} e_1. \end{aligned}$$

We further set

$$\begin{aligned} \tilde{\Delta} \hat{\mu}_{Z_{k+},l}(h_k) &\equiv \Delta \hat{\mu}_{Z_{k+},l}(h_k) - \sqrt{n}(h_k)^{3/2+l} B_{Z_{k+},l,l+1}(h_k), \\ \tilde{\Delta} \hat{\mu}_{Z_{k-},l}(h_k) &\equiv \Delta \hat{\mu}_{Z_{k-},l}(h_k) - \sqrt{n}(h_k)^{3/2+l} B_{Z_{k-},l,l+1}(h_k), \\ \tilde{\Delta} \hat{f}_{+,p}(h_f) &\equiv \Delta \hat{f}_{+,p}(h_f) - \sqrt{n} h_f^{p+1/2} B_{f,+ ,p,p+1}(h_f), \\ \tilde{\Delta} \hat{f}_{-,p}(h_f) &\equiv \Delta \hat{f}_{-,p}(h_f) - \sqrt{n} h_f^{p+1/2} B_{f,- ,p,p+1}(h_f), \end{aligned}$$

Using Lemmas A.1 and A.2, the following provides an asymptotic distribution for the local polynomial estimators.

**Lemma A.3.** *Suppose Assumptions 1–2 hold with  $S \geq l+2$  and  $R \geq p+1$ . If  $nh_{\min} \rightarrow \infty$ ,  $nh_f^2 \rightarrow \infty$ ,  $n(h_{\max})^{2l+5} \rightarrow 0$ , and  $n(h_f)^{2p+3} \rightarrow 0$ , then*

$$[\tilde{\Delta} \hat{\mu}_{Z_{1+},l}(h_1), \dots, \tilde{\Delta} \hat{\mu}_{Z_{d+},l}(h_d), \tilde{\Delta} \hat{f}_{+,p}(h_f)]' \xrightarrow{d} N_{d+1}(0, V_{+,l,p}), \quad (\text{A.10})$$

$$[\tilde{\Delta} \hat{\mu}_{Z_{1-},l}(h_1), \dots, \tilde{\Delta} \hat{\mu}_{Z_{d-},l}(h_d), \tilde{\Delta} \hat{f}_{-,p}(h_f)]' \xrightarrow{d} N_{d+1}(0, V_{-,l,p}), \quad (\text{A.11})$$

where

$$\begin{aligned} V_{+,l,p} &= \begin{pmatrix} V_{Z_{+,l}} & 0 \\ 0 & V_{f,+ ,p} \end{pmatrix}, & V_{Z_{+,l}} &= \{C_{Z_j Z_{k+},l}\}_{j,k=1,\dots,d}, \\ V_{-,l,p} &= \begin{pmatrix} V_{Z_{-,l}} & 0 \\ 0 & V_{f,- ,p} \end{pmatrix}, & V_{Z_{-,l}} &= \{C_{Z_j Z_{k-},l}\}_{j,k=1,\dots,d}. \end{aligned}$$

**Remark 5.** In Lemma A.2 (b), the results for the estimators on the left and right sides are not analogous. The term

$$\{-f_+^3 F_+ + f_+ f_+'(F_+ - F_+^2)\} \Gamma_p (e_1 e_0' + e_0 e_1') \Gamma_p$$

for the right-hand-side estimator changes to

$$-\{ -f_-^3(F_- - 1) + f_- f_-'(F_- - F_-^2) \} H_p(-1) \Gamma_p(e_1 e_0' + e_0 e_1') \Gamma_p H_p(-1)$$

for the left-hand-side estimator. Nevertheless, we observe the following.

$$e_1' \Gamma_p^{-1} \Gamma_p (e_1 e_0' + e_0 e_1') \Gamma_p \Gamma_p^{-1} e_1 = e_1' (e_1 e_0' + e_0 e_1') e_1 = 0,$$

and the difference has no effect on the asymptotic variances  $V_{f,+p}$  and  $V_{f,-p}$ . We outline the proof of Lemma A.2 (b) for the left-side estimator in Remark 6.

### A.3 Result for implementation

As mentioned in the main text, we implemented bias correction by increasing the order of the local polynomial estimators constructed from the following (not bias-corrected) distributional approximation.

**Theorem A.1.** *Suppose that Assumptions 1 and 2 hold, with  $R \geq p + 2$  and  $S \geq l + 3$ . If  $nh_{\min} \rightarrow \infty$ ,  $nh_f^2 \rightarrow \infty$ ,  $n(h_{\max})^{2l+5} \rightarrow 0$ , and  $n(h_f)^{2p+3} \rightarrow 0$ , then:*

$$\begin{aligned} & \sqrt{n} [\sqrt{h_1} (\hat{\tau}_{Z_1, l+1}(h_1) - \tau_{Z_1}), \dots, \sqrt{h_d} (\hat{\tau}_{Z_d, l+1}(h_d) - \tau_{Z_d}), \sqrt{h_f} (\hat{\tau}_{f, p+1}(h_f) - \tau_f)]' \\ & \xrightarrow{d} N_{d+1}(0, V_{l+1, p+1}). \end{aligned}$$

### A.4 Asymptotic covariance matrix and standard error estimation

Using the asymptotic covariance matrices of  $(\hat{\mu}_{Z_1, l}(h_1), \dots, \hat{\mu}_{Z_d, l}(h_d), \hat{f}_{+, p}(h_f))'$  and  $(\hat{\mu}_{Z_1, -l}(h_1), \dots, \hat{\mu}_{Z_d, -l}(h_d), \hat{f}_{-, p}(h_f))'$ , the asymptotic covariance matrix of  $(\hat{\tau}_{Z_1, l}(h_1), \dots, \hat{\tau}_{Z_d, l}(h_d), \hat{\tau}_{f, p}(h_f))'$  is

$$V_{l, p} = V_{+, l, p} + V_{-, l, p} = \begin{pmatrix} V_{Z, l} & 0 \\ 0 & V_{f, p} \end{pmatrix},$$

where  $V_{Z, l} = V_{Z_+, l} + V_{Z_-, l} = \{C_{Z_j Z_k, l} + C_{Z_j Z_k, -l}\}_{j, k=1, \dots, d}$  and  $V_{f, p} = V_{f, +, p} + V_{f, -, p}$ . We propose the following estimator for the asymptotic covariance matrix:

$$\hat{V}_{l, p}(h) = \hat{V}_{+, l, p}(h) + \hat{V}_{-, l, p}(h) = \begin{pmatrix} \hat{V}_{Z, l}(h) & 0 \\ 0 & \hat{V}_{f, p}(h_f) \end{pmatrix},$$

where  $\hat{V}_{Z,l}(h) = \hat{V}_{Z+,l}(h) + \hat{V}_{Z-,l}(h) = \{\hat{C}_{Z_j Z_{k+},l}(h_j, h_k) + \hat{C}_{Z_j Z_{k-},l}(h_j, h_k)\}_{j,k=1,\dots,d}$  and  $\hat{V}_{f,p}(h_f) = \hat{V}_{f+,p}(h_f) + \hat{V}_{f-,p}(h_f)$ .

For  $\hat{C}_{Z_j Z_{k+},l}(h_j, h_k)$  and  $\hat{C}_{Z_j Z_{k-},l}(h_j, h_k)$ , we follow an approach similar to the standard error estimators of Calonico et al. (2014) based on nearest-neighbor estimation. We define

$$\hat{C}_{Z_j Z_{k+},l}(h_j, h_k) = h_{jk} e_0' \Gamma_{+,l}^{-1}(h_j) \hat{\Psi}_{Z_j Z_{k+},l}(h_j, h_k) \Gamma_{+,l}^{-1}(h_k) e_0,$$

$$\hat{C}_{Z_j Z_{k-},l}(h_j, h_k) = h_{jk} e_0' \Gamma_{-,l}^{-1}(h_j) \hat{\Psi}_{Z_j Z_{k-},l}(h_j, h_k) \Gamma_{-,l}^{-1}(h_k) e_0$$

with

$$\hat{\Psi}_{Z_j Z_{k+},l}(h_j, h_k) = X_l(h_j)' W_+(h_j) \hat{\Sigma}_{Z_j Z_{k+}} W_+(h_k) X_l(h_k) / n,$$

$$\hat{\Psi}_{Z_j Z_{k-},l}(h_j, h_k) = X_l(h_j)' W_-(h_j) \hat{\Sigma}_{Z_j Z_{k-}} W_-(h_k) X_l(h_k) / n,$$

$$\hat{\Sigma}_{Z_j Z_{k+}} = \text{diag}(\hat{\sigma}_{Z_j Z_{k+}}^2(X_1), \dots, \hat{\sigma}_{Z_j Z_{k+}}^2(X_n)),$$

$$\hat{\Sigma}_{Z_j Z_{k-}} = \text{diag}(\hat{\sigma}_{Z_j Z_{k-}}^2(X_1), \dots, \hat{\sigma}_{Z_j Z_{k-}}^2(X_n)),$$

$$\hat{\sigma}_{Z_j Z_{k+}}^2(X_i) = 1\{X_i \geq 0\} \frac{M}{M+1} \left( Z_{j,i} - \sum_{m=1}^M \frac{Z_{j,l_m^+(i)}}{M} \right) \left( Z_{k,i} - \sum_{m=1}^M \frac{Z_{k,l_m^+(i)}}{M} \right),$$

$$\hat{\sigma}_{Z_j Z_{k-}}^2(X_i) = 1\{X_i < 0\} \frac{M}{M+1} \left( Z_{j,i} - \sum_{m=1}^M \frac{Z_{j,l_m^-(i)}}{M} \right) \left( Z_{k,i} - \sum_{m=1}^M \frac{Z_{k,l_m^-(i)}}{M} \right),$$

where  $l_m^+(i)$  and  $l_m^-(i)$  are the  $m$ th closest units to unit  $i$  among  $\{X_i : X_i \geq 0\}$  and  $\{X_i : X_i < 0\}$  respectively, and  $M$  denotes the number of neighbors. Calonico et al. (2014) shows that, if  $\sigma_{Z_j Z_k}^2(x)$  is Lipschitz continuous on  $(-\kappa_0, \kappa_0)$ , then, for any choice of  $M \in \mathbb{N}_+$ ,

$$\hat{\Psi}_{Z_j Z_{k+},l}(h_j, h_k) = \Psi_{Z_j Z_{k+},l}(h_j, h_k) + o_p(\min\{h_j^{-1}, h_k^{-1}\}),$$

$$\hat{\Psi}_{Z_j Z_{k-},l}(h_j, h_k) = \Psi_{Z_j Z_{k-},l}(h_j, h_k) + o_p(\min\{h_j^{-1}, h_k^{-1}\})$$

hold, which leads to  $\hat{V}_{Z,l}(h) \xrightarrow{P} V_{Z,l}$  combined with Lemma A.2.

For  $\hat{V}_{f,p}(h_f)$ , we employ the jackknife-based standard error estimator from Cattaneo et al. (2020), which may be more robust than plug-in estimations in finite samples. We define

$$\hat{V}_{f+,p}(h_f) = h_f^{-1} e_1' \Gamma_{+,p}^{-1}(h_f) \hat{\Psi}_{f+,p}(h_f) \Gamma_{+,p}^{-1}(h_f) e_1,$$

$$\hat{V}_{f-,p}(h_f) = h_f^{-1} e_1' \Gamma_{-,p}^{-1}(h_f) \hat{\Psi}_{f-,p}(h_f) \Gamma_{-,p}^{-1}(h_f) e_1,$$

with

$$\begin{aligned}
\hat{\Psi}_{f+,p}(h_f) &= \frac{1}{n} \sum_{i=1}^n \left( \frac{1}{n-1} \sum_{j:j \neq i}^n \hat{\phi}_{+,p,h_f}^*(X_i, X_j) \right) \left( \frac{1}{n-1} \sum_{j:j \neq i}^n \hat{\phi}_{+,p,h_f}^*(X_i, X_j) \right)' \\
&\quad - \left( \frac{1}{n(n-1)} \sum_{i,j:i < j}^n \hat{\phi}_{+,p,h_f}^*(X_i, X_j) \right) \left( \frac{1}{n(n-1)} \sum_{i,j:i < j}^n \hat{\phi}_{+,p,h_f}^*(X_i, X_j) \right)', \\
\hat{\Psi}_{f-,p}(h_f) &= \frac{1}{n} \sum_{i=1}^n \left( \frac{1}{n-1} \sum_{j:j \neq i}^n \hat{\phi}_{-,p,h_f}^*(X_i, X_j) \right) \left( \frac{1}{n-1} \sum_{j:j \neq i}^n \hat{\phi}_{-,p,h_f}^*(X_i, X_j) \right)' \\
&\quad - \left( \frac{1}{n(n-1)} \sum_{i,j:i < j}^n \hat{\phi}_{-,p,h_f}^*(X_i, X_j) \right) \left( \frac{1}{n(n-1)} \sum_{i,j:i < j}^n \hat{\phi}_{-,p,h_f}^*(X_i, X_j) \right)', \\
\hat{\phi}_{+,p,h_f}^*(X_i, X_j) &= \hat{\psi}_{+,p,h_f}^*(X_i, X_j) + \hat{\psi}_{+,p,h_f}^*(X_j, X_i), \\
\hat{\phi}_{-,p,h_f}^*(X_i, X_j) &= \hat{\psi}_{-,p,h_f}^*(X_i, X_j) + \hat{\psi}_{-,p,h_f}^*(X_j, X_i), \\
\hat{\psi}_{+,p,h_f}^*(X_i, X_j) &= 1\{X_i \geq 0\} r_p(X_i/h_f) (1\{X_j \leq X_i\} - r_p(X_i)' \hat{\beta}_{f+,p}(h_f)) K_{h_f}(X_i), \\
\hat{\psi}_{-,p,h_f}^*(X_i, X_j) &= 1\{X_i < 0\} r_p(X_i/h_f) (1\{X_j \leq X_i\} - r_p(X_i)' \hat{\beta}_{f-,p}(h_f)) K_{h_f}(X_i).
\end{aligned}$$

These estimators can be motivated from another representations of  $\Delta \hat{f}_{+,p}(h_f)$  and  $\Delta \hat{f}_{-,p}(h_f)$ . For  $\Delta \hat{f}_{+,p}(h_f)$ , one can show that

$$\Delta \hat{f}_{+,p}(h_f) = \sqrt{\frac{n}{h_f}} e_1' \Gamma_{+,p}^{-1}(h_f) U_{+,p}^*(h_f) + O_p\left(\frac{1}{\sqrt{nh_f}}\right),$$

where

$$U_{+,p}^*(h_f) = \frac{1}{n(n-1)} \sum_{i,j:i \neq j}^n \psi_{+,p,h_f}^*(X_i, X_j),$$

$$\psi_{+,p,h_f}^*(X_i, X_j) = 1\{X_i \geq 0\} r_p(X_i/h_f) (1\{X_j \leq X_i\} - r_p(X_i)' \beta_{f+,p}) K_{h_f}(X_i),$$

and  $\hat{\Psi}_{f+,p}(h_f)$  is constructed to approximate the asymptotic variance of the second-order U-statistic  $U_{+,p}^*(h_f)$ .

## A.5 Proof of the results

The proofs in this section use several auxiliary results (Lemma A.4) collected in Appendix A.6. For Lemmas A.1-A.3, we only provide proofs for the right-hand-side estimators ( $\hat{\mu}_{Z_k+,l}(h_k)$ ,  $\hat{f}_{+,p}(h_f)$ ), and the proofs of the left-hand-side estimators ( $\hat{\mu}_{Z_k-,l}(h_k)$  and  $\hat{f}_{-,p}(h_f)$ ) are analogous. Without loss of generality, we assume that

$\kappa h_j < \kappa_0$  for  $j = 1, \dots, d, f$  to bound the densities and error variances evaluated at  $uh_f$  where  $u \in (-\kappa, \kappa)$ .

*Proof of Lemma A.1.* For part (a), applying Lemma S.A.3 (B) of Calonico et al. (2014) to  $E[\hat{\mu}_{Z_k+l}(h_k)|\mathcal{X}_n]$  for  $k = 1, \dots, d$  yields:

$$\begin{aligned} & \frac{1}{\sqrt{n}} \Delta^B \hat{\mu}_{Z_k+l}(h_k) \\ &= (h_k)^{3/2+l} \frac{\mu_{Z_k+}^{(l+1)}}{(l+1)!} \mathcal{B}_{+,0,l,l+1}(h_k) + (h_k)^{5/2+l} \frac{\mu_{Z_k+}^{(l+2)}}{(l+2)!} \mathcal{B}_{+,0,l,l+2}(h_k) + o_p((h_k)^{5/2+l}). \end{aligned} \tag{A.12}$$

For  $\Delta^{B_0} \hat{f}_{+,p}(h_f)$  in part (b), a derivation analogous to the proof of Lemma 2 in Cattaneo et al. (2020) gives

$$\begin{aligned} & \frac{1}{\sqrt{n}} \Delta^{B_0} \hat{f}_{+,p}(h_f) \\ &= h_f^{p+1/2} \frac{f_+^{(p)}}{(p+1)!} \mathcal{B}_{+,1,p,p+1}(h_f) + h_f^{p+3/2} \frac{f_+^{(p+1)}}{(p+2)!} \mathcal{B}_{+,1,p,p+2}(h_f) + o_p((h_f)^{p+3/2}). \end{aligned} \tag{A.13}$$

For  $\Delta^{B_1} \hat{f}_{+,p}(h_f)$  in part (b), we observe that

$$\begin{aligned} & E \left[ \frac{1}{n} |X_p(h_f)' W_+(h_f)(\iota - F)| \right] \\ & \leq \frac{1}{n} \sum_{i=1}^n E \left[ |r_p(X_i/h_f)' 1\{X_i \geq 0\} K_{h_f}(X_i)(1 - F(X_i))| \right] \\ & \lesssim \int_0^\infty |r_p(u)| K(u) f(h_f u) = O(1), \end{aligned}$$

and using the Markov's inequality,

$$\frac{1}{n} X_p(h_f)' W_+(h_f)(\iota - F) = O_p(1).$$

Thus, we obtain  $\Delta^{B_1} \hat{f}_{+,p}(h_f) = O_p\left(\frac{1}{\sqrt{nh_f}}\right)$ .



For part (c), we observe the following.

$$\begin{aligned}
E[|U_{2,+p}(h_f)|^2] &\lesssim \frac{1}{n(n-1)} E[|\varphi_{+,p,h_f}(X_i, X_j)|^2] \\
&\lesssim \frac{1}{n(n-1)} E[|\psi_{+,p,h_f}(X_i, X_j) - E[\psi_{+,p,h_f}(X_i, X_j)|X_j]|^2] \\
&\quad + \frac{1}{n(n-1)} E[|\psi_{+,p,h_f}(X_j, X_i) - E[\psi_{+,p,h_f}(X_j, X_i)|X_i]|^2] \\
&\lesssim \frac{1}{n(n-1)} E[|\psi_{+,p,h_f}(X_i, X_j)|^2].
\end{aligned} \tag{A.14}$$

A derivation analogous to the proof of Lemma 4 in Cattaneo et al. (2020) provides

$$\begin{aligned}
&\frac{1}{n(n-1)} E[|\psi_{+,p,h_f}(X_i, X_j)|^2] \\
&\lesssim \frac{1}{n(n-1)h_f} f_+(F_+ - F_+^2) \int_0^\infty K(u)^2 r_p(u)' r_p(u) du + O\left(\frac{1}{n^2}\right) = O_p\left(\frac{1}{n^2 h_f}\right),
\end{aligned} \tag{A.15}$$

which implies that  $U_{2,+p}(h_f) = O_p\left(\frac{1}{n\sqrt{h_f}}\right)$  from Chebyshev's inequality. Hence part (c) follows from  $\sqrt{\frac{n}{h_f}} U_{2,+p}(h_f) = O_p\left(\frac{1}{\sqrt{nh_f^2}}\right)$ .  $\square$

*Proof of Lemma A.2.* Observe that

$$\begin{aligned}
&\text{Cov}\left(\sqrt{\frac{h_j}{n}} X_l(h_j)' W_+(h_j) \varepsilon_{Z_j}, \sqrt{\frac{h_k}{n}} X_l(h_k)' W_+(h_k) \varepsilon_{Z_k} | \mathcal{X}_n\right) \\
&= \frac{h_{jk}}{n} X_l(h_j)' W_+(h_j) \Sigma_{Z_j Z_k} W_+(h_k) X_l(h_k) = h_{jk} \Psi_{Z_j Z_k +, l, l}(h_j, h_k)
\end{aligned}$$

and part (a) follows from Lemma A.4 (a).

Note that

$$\begin{aligned}
&E[\psi_{+,p,h_f}(X_j, X_i) | X_i] \\
&= \int_0^\infty r_p(u) (1(X_i \leq h_f u) - F(h_f u)) K(u) f(h_f u) du,
\end{aligned}$$

A derivation analogous to the proof of Lemma 3 in Cattaneo et al. (2020) provides

$$\begin{aligned}
& \text{Var} \left( \int_0^\infty r_p(u) (1(X_i \leq h_f u) - F(h_f u)) K(u) f(h_f u) du \right) \\
&= \int_0^\infty \int_0^\infty r_p(u) r_p(v)' K(u) K(v) f(h_f u) f(h_f v) \{F(h_f(u \wedge v)) - F(h_f u) F(h_f v)\} dudv \\
&= f_+^2 (F_+ - F_+^2) \int_0^\infty \int_0^\infty r_p(u) r_p(v)' K(u) K(v) dudv + h_f f_+^3 \Psi_{f,p} \\
&\quad + h_f \{-f_+^3 F_+ + f_+ f'_+(F_+ - F_+^2)\} \int_0^\infty \int_0^\infty (u+v) r_p(u) r_p(v)' K(u) K(v) dudv + o(1),
\end{aligned}$$

Hence, part (b) follows from

$$\int_0^\infty r_p(u) K(u) du = \Gamma_p e_0 \quad \text{and} \quad \int_0^\infty u r_p(u) K(u) du = \Gamma_p e_1.$$

Observe that

$$X_l(h_k)' W_+(h_k) \varepsilon_{Z_k} = \sum_{i=1}^n 1\{X_i \geq 0\} K_{h_k}(X_i) r_l(X_i/h_k) \varepsilon_{Z_k,i}$$

and part (c) follows from

$$\begin{aligned}
& \text{Cov} \left( \sum_{i=1}^n 1\{X_i \geq 0\} K_{h_k}(X_i) r_l(X_i/h_k) \varepsilon_{Z_k,i}, \sum_{i=1}^n E[\psi_{+,p,h_f}(X_j, X_i) | X_i] \right) \\
&= \sum_{i=1}^n E \left[ 1\{X_i \geq 0\} K_{h_k}(X_i) r_l(X_i/h_k) \varepsilon_{Z_k,i} E[\psi_{+,p,h_f}(X_j, X_i) | X_i] \right] = 0
\end{aligned}$$

because  $E[\varepsilon_{Z_k,i} | \mathcal{X}_n] = 0$ . □

**Remark 6.** We now outline the proof of Lemma A.2 (b) for the left-hand-side estimator. A derivation analogous to the proof for the right-side estimator yields

$$\begin{aligned}
& \text{Var} \left( E[\psi_{-,p,h_f}(X_j, X_i) | X_i] \right) \\
&= f_-^2 (F_- - F_-^2) H_p(-1) \int_0^\infty \int_0^\infty r_p(u) r_p(v)' K(u) K(v) dudv H_p(-1) \\
&\quad + h_f f_-^3 H_p(-1) \int_0^\infty \int_0^\infty \{(-u) \wedge (-v)\} r_p(u) r_p(v)' K(u) K(v) dudv H_p(-1) \\
&\quad + h_f \{-f_-^3 F_- + f_- f'_-(F_- - F_-^2)\} \\
&\quad \times H_p(-1) \int_0^\infty \int_0^\infty -(u+v) r_p(u) r_p(v)' K(u) K(v) dudv H_p(-1) + o(1),
\end{aligned}$$

and the stated result follows from

$$(-u) \wedge (-v) = \frac{1}{2}(-u - v - |u - v|) = u \wedge v - (u + v).$$

*Proof of Lemma A.3.* We show that

$$\sum_{k=1}^d t_k \tilde{\Delta} \hat{\mu}_{Z_k+l}(h_k) + t_f \tilde{\Delta} \hat{f}_{+,p} \xrightarrow{d} N(0, \tilde{t}' V_{+,l,p} \tilde{t}), \quad (\text{A.16})$$

The stated result follows from the Cramér-Wold theorem.

We set

$$\xi_{1,n} = \sum_{k=1}^d t_k \Delta^M \hat{\mu}_{Z_k+l}(h_k) + t_f \Delta^M \hat{f}_{+,p}(h_f) \quad (\text{A.17})$$

and

$$\xi_{2,n} = \sum_{k=1}^d t_k \tilde{\Delta}^B \hat{\mu}_{Z_k+l}(h_k) + t_f \tilde{\Delta}^B \hat{f}_{+,p}(h_f), \quad (\text{A.18})$$

where

$$\tilde{\Delta}^B \hat{\mu}_{Z_k+l}(h_k) \equiv \Delta^B \hat{\mu}_{Z_k+l}(h_k) - \sqrt{n}(h_k)^{3/2+l} B_{Z_k+l,l+1}(h_k)$$

and

$$\tilde{\Delta}^B \hat{f}_{+,p}(h_f) \equiv \Delta^B \hat{f}_{+,p}(h_f) - \sqrt{n} h_f^{p+1/2} B_{f,+,p,p+1}(h_f).$$

To demonstrate (A.16), we decompose the left-hand-side as follows.

$$\sum_{k=1}^d t_k \tilde{\Delta} \hat{\mu}_{Z_k+l}(h_k) + t_f \tilde{\Delta} \hat{f}_{+,p}(h_f) = \xi_{1,n} + \xi_{2,n}.$$

We show that  $\xi_{1,n} \xrightarrow{d} N(0, \tilde{t}' V_{+,l,p} \tilde{t})$  and  $\xi_{2,n} = o_p(1)$ .

First, we demonstrate that  $\xi_{2,n} = o_p(1)$ . If  $h_{max} \rightarrow 0$ , then from Lemma A.1 (a),

$$\sum_{k=1}^d t_k \tilde{\Delta}^B \hat{\mu}_{Z_k+l}(h_k) = O_p \left( \sqrt{n} \sum_{k=1}^d (h_k)^{5/2+l} \right) = O_p \left( \sqrt{n} (h_{max})^{5/2+l} \right). \quad (\text{A.19})$$

From Lemma A.2 (b),  $E[|\sqrt{\frac{n}{h_f}} U_{1,+,p}(h_f)|^2] = O(\frac{1}{h_f})$ , implying

$\sqrt{\frac{n}{h_f}} U_{1,+,p}(h_f) = O_p(\frac{1}{\sqrt{h_f}})$  from Chebyshev's inequality. Hence, we have  $\Delta^{B_3} \hat{f}_{+,p}(h_f) = O_p(\frac{1}{n\sqrt{h_f}})$  and

$$\tilde{\Delta}^B \hat{f}_{+,p}(h_f) = O_p \left( \sqrt{n} h_f^{3/2+p} \right) + O_p \left( \frac{1}{\sqrt{n h_f^2}} \right).$$

Therefore, we have  $\xi_{2,n} = o_p(1)$  for the bias.

Next, we demonstrate that  $\xi_{1,n} \xrightarrow{d} N(0, 1)$ . Let

$$\tilde{\Delta}^M \hat{\mu}_{Z_k+,l}(h_k) = \sqrt{\frac{h_k}{n}} f_+^{-1} e_0' \Gamma_l^{-1} X_l(h_k)' W_+(h_k) \varepsilon_{Z_k}$$

and

$$\tilde{\Delta}^M \hat{f}_{+,p}(h_f) = \sqrt{\frac{n}{h_f}} f_+^{-1} e_1' \Gamma_p^{-1} U_{1,+,p}(h_f).$$

Subsequently, we have

$$\Delta^M \hat{\mu}_{Z_k+,l}(h_k) = \tilde{\Delta}^M \hat{\mu}_{Z_k+,l}(h_k) + o_p(1)$$

and

$$\Delta^M \hat{f}_{+,p}(h_f) = \tilde{\Delta}^M \hat{f}_{+,p}(h_f) + O_p \left( \sqrt{h_f} + \frac{1}{\sqrt{nh_f^2}} \right).$$

To demonstrate this, from Lemma S.A.1 in Calonico et al. (2014), we obtain

$$\Gamma_{+,p}(h_f) = f_+ \Gamma_p + O_p \left( h_f + \frac{1}{\sqrt{nh_f}} \right),$$

Hence,  $|\Gamma_{+,p}(h_f) - f_+ \Gamma_p| < 1$  with a probability approaching one. Consequently, a well-known result for the matrix inverse yields

$$|\Gamma_{+,p}^{-1}(h_f) - f_+^{-1} \Gamma_p^{-1}| \leq \frac{|\Gamma_{+,p}(h_f) - f_+ \Gamma_p| |f_+^{-1} \Gamma_p^{-1}|^2}{1 - |\Gamma_{+,p}(h_f) - f_+ \Gamma_p| |f_+^{-1} \Gamma_p^{-1}|} = O_p \left( h_f + \frac{1}{\sqrt{nh_f}} \right)$$

with a probability approaching one. Hence, we obtain

$$\Gamma_{+,p}^{-1}(h_f) = f_+^{-1} \Gamma_p^{-1} + O_p \left( h_f + \frac{1}{\sqrt{nh_f}} \right),$$

and we have  $\sqrt{\frac{h_k}{n}} X_l(h_k)' W_+(h_k) \varepsilon_{Z_k} = O_p(1)$  and  $\sqrt{\frac{n}{h_f}} U_{1,+,p}(h_f) = O_p \left( \frac{1}{\sqrt{h_f}} \right)$  from Lemma A.2 (a) and (b), respectively. Let

$$\tilde{\xi}_{1,n} = \sum_{k=1}^d t_k \tilde{\Delta}^M \hat{\mu}_{Z_k+,l}(h_k) + t_f \tilde{\Delta}^M \hat{f}_{+,p}(h_f).$$

Subsequently, from the previous definitions and derivations,  $\xi_{1,n} = \tilde{\xi}_{1,n} + o_p(1)$ .

Thus, it remains to show that  $\tilde{\xi}_{1,n} \xrightarrow{d} N(0, \tilde{t}' V_{+,l,p} \tilde{t})$ . Notably,  $\tilde{\xi}_{1,n}$  can be represented

as  $\tilde{\xi}_{1,n} = \sum_{i=1}^n \hat{\omega}_i$  with

$$\hat{\omega}_i \equiv f_+^{-1} \left\{ e'_0 \Gamma_l^{-1} \sum_{k=1}^d t_k \hat{\omega}_{k,i} \varepsilon_{Z_k,i} + t_f e'_1 \Gamma_p^{-1} \hat{\omega}_{f,i} \right\},$$

where

$$\hat{\omega}_{k,i} \equiv \sqrt{\frac{h_k}{n}} \mathbf{1}\{X_i \geq 0\} K_{h_k}(X_i) r_l(X_i/h_k)$$

and

$$\hat{\omega}_{f,i} \equiv \frac{1}{\sqrt{nh_f}} E[\psi_{+,p,h_f}(X_j, X_i) | X_i].$$

$\{\hat{\omega}_i\} : 1 \leq i \leq n$  denotes a triangular array of independent random variables; We show that

$$E[\tilde{\xi}_{1,n}] = 0, \tag{A.20}$$

$$\text{Var}(\tilde{\xi}_{1,n}) = \tilde{t}' V_{+,l,p} \tilde{t} + o(1), \tag{A.21}$$

and

$$\sum_{i=1}^n E[|\hat{\omega}_i|^4] = o(1). \tag{A.22}$$

The Lyapunov Condition—a well-known sufficient condition for the Lindeberg condition—is satisfied by (A.22). Therefore, from (A.20), (A.21), and (A.22), applying the Lindeberg-Feller central limit theorem yields that  $\tilde{\xi}_{1,n} \xrightarrow{d} N(0, \tilde{t}' V_{+,l,p} \tilde{t})$  (see, for example, Durrett (2019)).

First, from the definition, (A.20) follows from  $E[\varepsilon_{Z_k,i} | \mathcal{X}_n] = 0$  and  $E[\psi_{+,p,h_f}(X_j, X_i)] = 0$ . Next, from Lemmas A.2 (a) and (b), we have

$$\begin{aligned} \text{Var}(\tilde{\xi}_{1,n}) &= \text{Var} \left( \sum_{k=1}^d t_k \tilde{\Delta}^M \hat{\mu}_{Z_k+,l}(h_k) \right) + \text{Var} \left( t_f \tilde{\Delta}^M \hat{f}_{+,p}(h_f) \right) \\ &= t' V_{Z+,l} t + t_f^2 V_{f+,p} + o(1). \end{aligned}$$

Hence, we obtain (A.21). Finally, similar to the proof of Lemma S.A.3 (D) in Calonico et al. (2014), we obtain

$$\begin{aligned} \sum_{i=1}^n E[|\hat{\omega}_{k,i} \varepsilon_{Z_k,i}|^4] &\lesssim \sum_{i=1}^n E[|\hat{\omega}_{k,i}|^4] \\ &\lesssim \frac{1}{nh_k} \int_0^\infty K(u)^4 |r_p(u)|^4 f(h_k u) du = O\left(\frac{1}{nh_k}\right). \end{aligned}$$

The first inequality holds because, for two random variables  $W$  and  $Y$ ,  $E[|W +$

$Y^4|X_i = x] \leq 8\{E[W^4|X_i = x] + E[Y^4|X_i = x]\}$  holds,

$$E[\varepsilon_{Z_{k,i}}^4|X_i = x] \leq 8\{E[|Z_{k,i}|^4|X_i = x] + \mu(x)^4\}. \quad (\text{A.23})$$

Hence,  $E[\varepsilon_{Z_{k,i}}^4|X_i = x]$  is bounded, based on Assumption 1. Similar to the proof of Lemma 3 in Cattaneo et al. (2020), we obtain

$$\begin{aligned} & \sum_{i=1}^n E[|\hat{\omega}_{f,i}|^4] \\ & \lesssim \int_0^\infty \int_0^\infty \int_0^\infty \int_0^\infty r_p(u_1)r_p(u_2)'r_p(u_3)r_p(u_4)' \prod_{j=1}^4 [K(u_j)f(h_f u_j)] du_1 du_2 du_3 du_4 \\ & = O\left(\frac{1}{nh_f^2}\right). \end{aligned}$$

Observe that

$$\begin{aligned} & \sum_{i=1}^n E[|\hat{\omega}_{f,i}|^4] \lesssim \sum_{i=1}^n \sum_{k=1}^d E[|t_k \hat{\omega}_{k,i \in Z_{k,i}}|^4] + \sum_{i=1}^n E[|t_f \hat{\omega}_{f,i}|^4] \\ & \lesssim \sum_{k=1}^d \sum_{i=1}^n E[|\hat{\omega}_{k,i \in Z_{k,i}}|^4] + \sum_{i=1}^n E[|\hat{\omega}_{f,i}|^4] \\ & \lesssim O\left(\frac{1}{nh_{\min}}\right) + O\left(\frac{1}{nh_f^2}\right). \end{aligned} \quad (\text{A.24})$$

The first inequality in (A.24) holds because, for two random variables  $W$  and  $Y$ ,  $E[|W + Y|^4] \leq 8\{E[W^4] + E[Y^4]\}$  holds iteratively. Therefore, (A.22) follows.  $\square$

*Proof of Theorem 3.1.* The stated result follows from the same argument given in the proof of Lemma A.3 using the analogs of Lemmas A.1 and A.2, but is now applied to the estimator  $(\hat{\tau}_{Z_1,l}(h_1), \dots, \hat{\tau}_{Z_d,l}(h_d), \hat{\tau}_{f,p}(h_f))'$ .  $\square$

*Proof of Theorem A.1.* Under the same assumption as in Theorem A.1, the asymptotic distribution for the local polynomial estimators, where the order is increased instead of eliminating the bias term, is as follows.

$$\begin{aligned} & [\Delta \hat{\mu}_{Z_1+l+1}(h_1), \dots, \Delta \hat{\mu}_{Z_d+l+1}(h_d), \Delta \hat{f}_{+,p+1}(h_f)]' \xrightarrow{d} N_{d+1}(0, V_{+,l+1,p+1}), \\ & [\Delta \hat{\mu}_{Z_1-l+1}(h_1), \dots, \Delta \hat{\mu}_{Z_d-l+1}(h_d), \Delta \hat{f}_{-,p+1}(h_f)]' \xrightarrow{d} N_{d+1}(0, V_{-,l+1,p+1}). \end{aligned}$$

This result and the stated result follow from a similar argument given in the proof of Lemma A.3 using the analogs of Lemmas A.1 and A.2.  $\square$

## A.6 Auxiliary Lemma

The following lemma establishes convergence in the probability of the sample matrix  $\Psi_{Z_j Z_{k+}, p, q}(h_j, h_k)$  to its population counterpart and characterizes this limit.

**Lemma A.4.** *Suppose that Assumptions 1-2 hold. If  $h_{jk} \rightarrow 0$  and  $nh_{jk} \rightarrow \infty$ , then*

$$h_{jk} \Psi_{Z_j Z_{k+}, p, q}(h_j, h_k) = \tilde{\Psi}_{Z_j Z_{k+}, p, q}(h_j, h_k) + o_p(1), \quad (\text{A.25})$$

$$h_{jk} \Psi_{Z_j Z_{k-}, p, q}(h_j, h_k) = H_p(-1) \tilde{\Psi}_{Z_j Z_{k-}, p, q}(h_j, h_k) H_q(-1) + o_p(1), \quad (\text{A.26})$$

and

$$\tilde{\Psi}_{Z_j Z_{k+}, p, q}(h_j, h_k) = \sigma_{Z_j Z_{k+}}^2 f_+ \Psi_{jk, p, q} + o(1), \quad (\text{A.27})$$

$$\tilde{\Psi}_{Z_j Z_{k-}, p, q}(h_j, h_k) = \sigma_{Z_j Z_{k-}}^2 f_- \Psi_{jk, p, q} + o(1). \quad (\text{A.28})$$

**Remark 7.** In the proof of Lemma A.4, we use the compactness of the support of  $K(\cdot)$  in the derivation of (A.27). We obtain (A.27) without assuming compactness in support of  $K(\cdot)$ . If  $\rho_{jk} \rightarrow c_{jk} \in (0, \infty)$ , (A.27) follows: continuity of  $K(u)$ ,  $r_p(u)$ ,  $\sigma_{Z_j Z_k}^4(u)$ , and  $f(u)$ . For the other cases, we observe the following.

$$\begin{aligned} & \tilde{\Psi}_{Z_j Z_{k+}, p, q}(h_j, h_k) \\ &= \frac{1}{h_{jk}} \int_0^\infty K\left(\frac{x}{h_j}\right) K\left(\frac{x}{h_k}\right) r_p\left(\frac{x}{h_j}\right) r_q\left(\frac{x}{h_k}\right)' \sigma_{Z_j Z_k}^2(x) f(x) dx \\ &= \frac{m_{jk}}{h_{jk}} \int_0^\infty K\left(\frac{m_{jk}u}{h_j}\right) K\left(\frac{m_{jk}u}{h_k}\right) r_p\left(\frac{m_{jk}u}{h_j}\right) r_q\left(\frac{m_{jk}u}{h_k}\right)' \sigma_{Z_j Z_k}^2(um_{jk}) f(um_{jk}) du. \end{aligned} \quad (\text{A.29})$$

Suppose that  $\rho_{jk, n} \rightarrow 0$ . Subsequently,  $h_{k, n} < h_{j, n}$ ; thus,  $m_{jk, n}/h_{jk, n} = \rho_{jk, n}^{1/2}$  holds for a sufficiently large  $n$ . Hence,  $m_{jk, n}/h_{jk, n} \rightarrow 0$ , and (A.27) follows from (A.29). The case of  $\rho_{jk, n}^{-1} \rightarrow 0$  follows from an analogous argument.

*Proof of Lemma A.4.* First, for  $\Psi_{Z_j Z_{k+}, p, q}(h_j, h_k)$ , a change in the variables yields

$$\begin{aligned}
& E[h_{jk} \Psi_{Z_j Z_{k+}, p, q}(h_j, h_k)] \\
&= E \left[ \frac{1}{nh_{jk}} \sum_{i=1}^n 1(X_i \geq 0) K \left( \frac{X_i}{h_j} \right) K \left( \frac{X_i}{h_k} \right) r_p \left( \frac{X_i}{h_j} \right) r_q \left( \frac{X_i}{h_k} \right)' \sigma_{Z_j Z_k}^2(X_i) \right] \\
&= \frac{1}{h_{jk}} \int_0^\infty K \left( \frac{x}{h_j} \right) K \left( \frac{x}{h_k} \right) r_p \left( \frac{x}{h_j} \right) r_q \left( \frac{x}{h_k} \right)' \sigma_{Z_j Z_k}^2(x) f(x) dx \\
&= \int_0^\infty K \left( \frac{h_{jk}u}{h_j} \right) K \left( \frac{h_{jk}u}{h_k} \right) r_p \left( \frac{h_{jk}u}{h_j} \right) r_q \left( \frac{h_{jk}u}{h_k} \right)' \sigma_{Z_j Z_k}^2(uh_{jk}) f(uh_{jk}) du \\
&= \tilde{\Psi}_{Z_j Z_{k+}, p, q}(h_j, h_k).
\end{aligned} \tag{A.30}$$

Let

$$\psi_{j,k,i} = 1(X_i \geq 0) K \left( \frac{X_i}{h_j} \right) K \left( \frac{X_i}{h_k} \right) r_p \left( \frac{X_i}{h_j} \right) r_q \left( \frac{X_i}{h_k} \right)' \sigma_{Z_j Z_k}^2(X_i), \tag{A.31}$$

where  $\psi_{j,k,i} = \{\psi_{j,k,l,m,i}\}_{l=1, \dots, (p+1)}^{m=1, \dots, (q+1)}$  is a  $(p+1) \times (q+1)$ -matrix. Additionally, let  $\psi_{j,k,l,m} = \sum_{i=1}^n \psi_{j,k,l,m,i}$  and  $\psi_{j,k} = \sum_{i=1}^n \psi_{j,k,i}$ . Observe that

$$\begin{aligned}
& h_{jk}^2 E[|\Psi_{Z_j Z_{k+}, p, q}(h_j, h_k) - E[\Psi_{Z_j Z_{k+}, p, q}(h_j, h_k)]|^2] \\
&= \frac{1}{n^2 h_{jk}^2} E[|\psi_{j,k} - E[\psi_{j,k}]|^2] = \frac{1}{n^2 h_{jk}^2} \sum_{l=1}^{p+1} \sum_{m=1}^{q+1} \text{Var}(\psi_{j,k,l,m}) \\
&= \frac{1}{n^2 h_{jk}^2} \sum_{l=1}^{p+1} \sum_{m=1}^{q+1} \sum_{i=1}^n \text{Var}(\psi_{j,k,l,m,i}) \\
&\leq \frac{1}{n^2 h_{jk}^2} \sum_{l=1}^{p+1} \sum_{m=1}^{q+1} \sum_{i=1}^n E[\psi_{j,k,l,m,i}^2] = \frac{1}{n^2 h_{jk}^2} \sum_{i=1}^n E[|\psi_{j,k,i}|^2]
\end{aligned} \tag{A.32}$$



and

$$\begin{aligned}
& \frac{1}{n^2 h_{jk}^2} \sum_{i=1}^n E[|\psi_{j,k,i}|^2] \\
&= \frac{1}{n h_{jk}^2} \int_0^\infty K\left(\frac{x}{h_j}\right)^2 K\left(\frac{x}{h_k}\right)^2 \left|r_p\left(\frac{x}{h_j}\right)\right|^2 \left|r_q\left(\frac{x}{h_k}\right)\right|^2 \sigma_{Z_j Z_k}^4(x) f(x) dx \\
&\leq \frac{1}{n m_{jk}^2} \int_0^\infty K\left(\frac{x}{h_j}\right)^2 K\left(\frac{x}{h_k}\right)^2 \left|r_p\left(\frac{x}{h_j}\right)\right|^2 \left|r_q\left(\frac{x}{h_k}\right)\right|^2 \sigma_{Z_j Z_k}^4(x) f(x) dx \\
&= \frac{1}{n m_{jk}} \int_0^\infty K\left(\frac{m_{jk}u}{h_j}\right)^2 K\left(\frac{m_{jk}u}{h_k}\right)^2 \\
&\quad \left|r_p\left(\frac{m_{jk}u}{h_j}\right)\right|^2 \left|r_q\left(\frac{m_{jk}u}{h_k}\right)\right|^2 \sigma_{Z_j Z_k}^4(um_{jk}) f(um_{jk}) du \\
&= O\left(\frac{1}{n m_{jk}}\right) = o(1).
\end{aligned} \tag{A.33}$$

Thus, (A.25) follows the Markov inequality. Second, (A.27) follows by continuity of  $K(u)$ ,  $r_p(u)$ ,  $\sigma_{Z_j Z_k}^4(u)$ , and  $f(u)$ , and the compactness of the support of  $K(\cdot)$ .  $\square$

## B Details on the search criterion

For the meta-analysis, we analyzed RD studies using diagnostic tests. There are two widely cited methodological papers, (McCrary, 2008 and Lee, 2008), and two widely cited survey papers, (Imbens and Lemieux, 2008 and Lee and Lemieux, 2010). We collected the citations of 2,697 unique papers on November 5, 2021, from the Web of Science.<sup>16</sup> Among 2,697 papers, we limited our focus to publications from the top five journals in economics (*American Economic Review*, *Econometrica*, *Journal of Political Economy*, *Quarterly Journal of Economics*, *Review of Economic Studies* in alphabetical order.). Among 98 in the top five publications, 60 papers reported at least one diagnostic test to validate their empirical analyses of RD designs. We excluded surveys, theoretical contributions, and other uses of similar tests in manipulation detection or kink designs. Furthermore, we limited our focus to the density and balance or placebo tests in their *standard* procedures, excluding placebo or balance tests for predicted variables from covariates. We identified five studies that incorporated a

<sup>16</sup>We used the Web of Science to limit our focus on published papers.

joint test for multiple testing problems. However, we did not include these joint tests because all but one study did not incorporate the nonparametric nature of the RD estimates. The only considered study (Fort et al., 2020) used Canay and Kamat (2018).

From these 60 papers, we collected the balance, placebo, or density test results that appeared to be their *main* specifications. In practice, many researchers have run multiple versions of these tests using different bandwidths, kernels, and specifications. We collected the total number of tests separately, but our numerical analysis was limited to the main specifications. We computed p-values from the reported statistics when only the test statistics were reported.

## C Details on the simulation data generating process

We conducted 3,000 replications to generate a random sample.

$$\{(X_i^+, X_i^-, \tilde{Z}_{1,i}, \dots, \tilde{Z}_{d,i}, U_i)' : i = 1, \dots, n\}$$

with size  $n = 500, 1000$ ,  $X_i^+ \sim tN(0, 0.12^2; [0, 1])$  with  $tN(\mu, \sigma^2; [0, 1])$  denotes a truncated normal distribution with mean  $\mu$  and variance  $\sigma^2$ , lying within the interval  $[0, 1]$ ,  $X_i^- \stackrel{d}{=} -X_i^+$ .  $U_i \sim Unif[0, 1]$  with  $Unif[0, 1]$  denoting a uniform distribution on the interval  $[0, 1]$ ,  $(\tilde{Z}_{1,i}, \dots, \tilde{Z}_{d,i})' \sim N_d(0, \tilde{\Sigma})$  with  $\tilde{\Sigma}$  denoting a correlation matrix where each  $(j, k)$  entry is  $1 > \rho \geq 0$  for  $j \neq k$ , and  $(X_i^+, X_i^-)$ ,  $(\tilde{Z}_{1,i}, \dots, \tilde{Z}_{d,i})$ , and  $U_i$  are mutually independent. The running variable  $X_i$  is generated as follows.

$$X_i = (1 - M_i)X_i^- + M_iX_i^+,$$

where  $M_i = 1\{U_i \leq \bar{p}\}$  with  $\bar{p} \geq 0.5$ . For pre-treatment covariates  $Z_i = (Z_{1,i}, \dots, Z_{d,i})'$ , we consider two specifications: first, one of the  $d$  covariates sees a jump, and second, all the  $d$  covariates see a jump, but each jump size is divided by  $d$ . For the first specification, each  $Z_{k,i}$ ,  $k = 1, \dots, d$  is generated as follows.

$$Z_{k,i} = \begin{cases} \lambda(X_i) + \tilde{Z}_{k,i} & \text{for } k = 1, \dots, d-1 \\ \lambda(X_i) + aM_i + \tilde{Z}_{k,i} & \text{for } k = d \text{ with } a \geq 0, \end{cases}$$

where the functional form of  $\lambda(x)$  is defined as

$$\lambda(x) = 0.48 + \begin{cases} 0.84x - 3.00x^2 + 7.99x^3 - 9.01x^4 + 3.56x^5, & \text{if } x \geq 0 \\ 1.27x + 7.18x^2 + 20.21x^3 + 21.54x^4 + 7.33x^5, & \text{otherwise.} \end{cases}$$

For the second specification, each  $Z_{k,i}, k = 1, \dots, d$  is generated as follows.

$$Z_{k,i} = \lambda(X_i) + a/dM_i + \tilde{Z}_{k,i}.$$

Let  $f^*(x)$  be the density of  $X_i^+$ ,

$$f^*(x) = \frac{\phi(x/0.12)}{0.12(\Phi(1/0.12) - \Phi(0))},$$

where  $\phi(x)$  and  $\Phi(x)$  are the density and cumulative distribution functions, respectively, of the standard normal random variable. Using  $f^*(x)$ , the density of  $X_i$  can be expressed as

$$f(x) = \begin{cases} f^*(x)(1 - \bar{p}) & \text{if } x < 0 \\ f^*(x)\bar{p} & \text{if } x > 0, \end{cases}$$

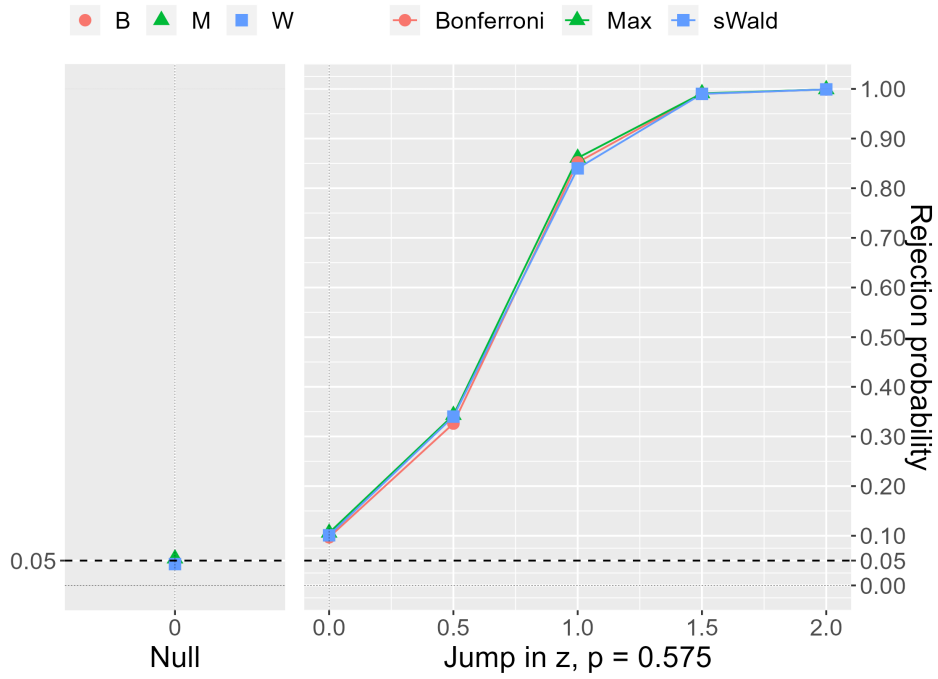
and the discontinuity level of  $f(x)$  at  $x = 0$  is  $\tau_f = f^*(0)(2\bar{p} - 1)$ . Hence, we have  $\tau_f = 0$  if and only if  $\bar{p} = 0.5$ , and  $\tau_f > 0$  when  $\bar{p} > 0.5$ .

## D Additional figures and tables

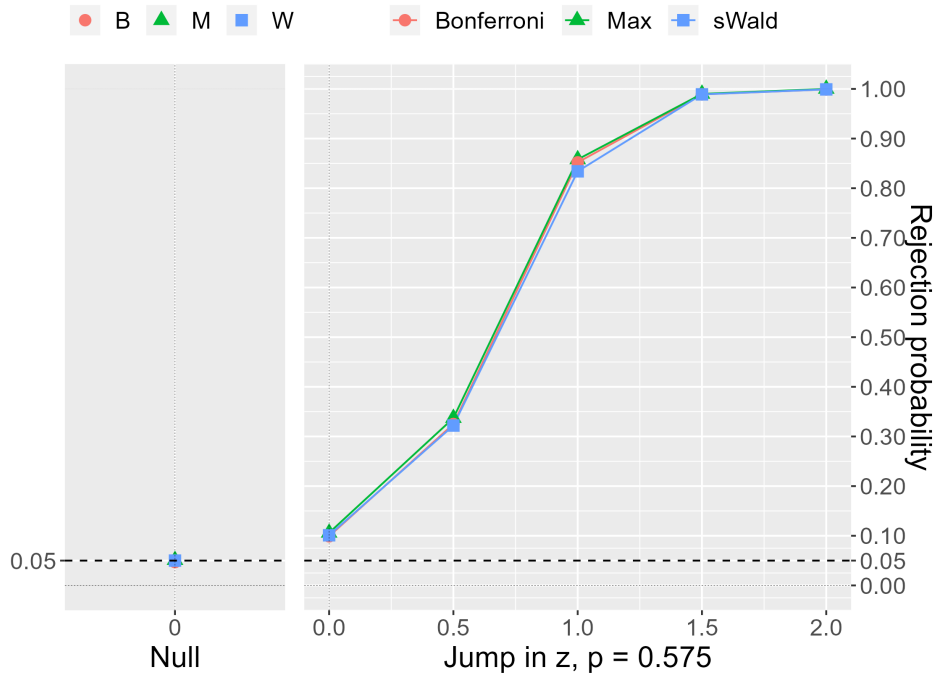
Figures 9-14 present the empirical power of the (ii) Bonferroni correction, (iv) Max test, and (v) sWald test under  $p = 0.575$  and  $\tau_{Z_d}(= a) = 0, 0.5, 1, 1.5, 2$  for different dimensions, and  $d = 3, 5$  for the Monte Carlo experiment in Section 4. In Figures 9–12, each figure presents the results for different correlations,  $\rho = 0, 0.3$ , which are weaker than those in Figures 5–8. Figures 9 and 10 present the results when one of the  $d$  covariates jumps, and Figures 11 and 12 present the results when all  $d$  covariates jump. However, each jump size is divided by  $d$  for  $d = 3, 5$ . Although the difference between the Max test and Bonferroni correction is smaller, the simulation results show that the proposed joint testing methods exhibit power improvements similar to those shown in Section 4. Moreover, the power improvements in the sWald test are more significant when the correlation is weaker.

Figures 13 and 14 compare the results for positive and negative correlations when  $d = 3$  and  $|\rho| = 0.9$ . In Figures 13 (b), and 14 (b), two of the three covariates have the

same pairwise correlation coefficient of 0.9, and the remaining one has the pairwise correlation coefficient of  $-0.9$ . Figure 13 presents the results when one of the three covariates jumps, and Figure 14 presents the results when all the three covariates jump. Nevertheless, each jump size is divided by three. Although the sWald test is conservative when the correlation is strong, the Max test had more power than the Bonferroni correction in both cases. This suggests that the power improvements in the Max test are robust against negative correlations.

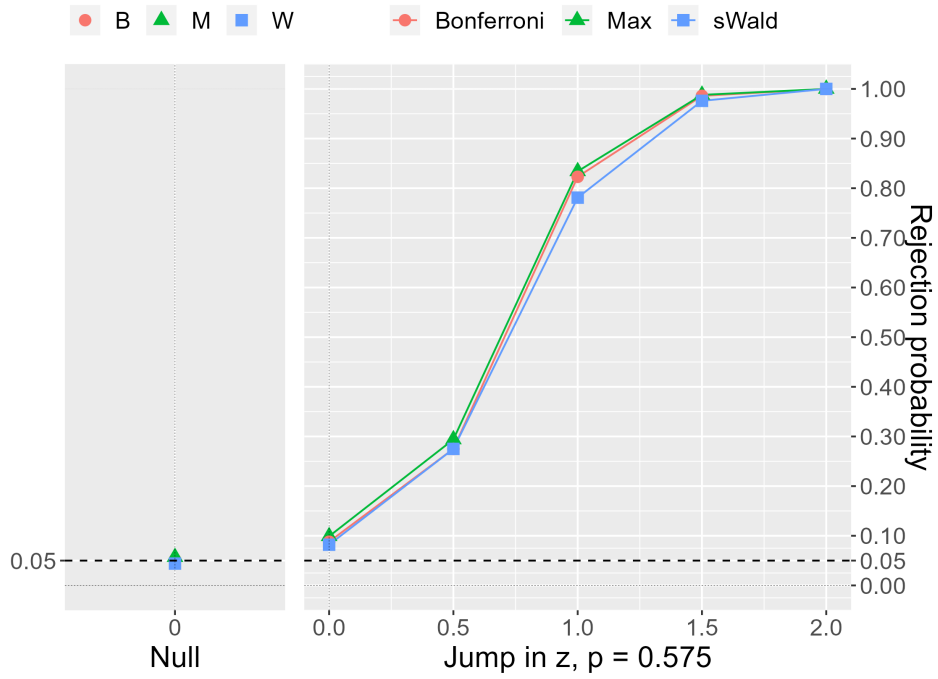


(a) Covariates have the same pairwise correlation coefficient of 0

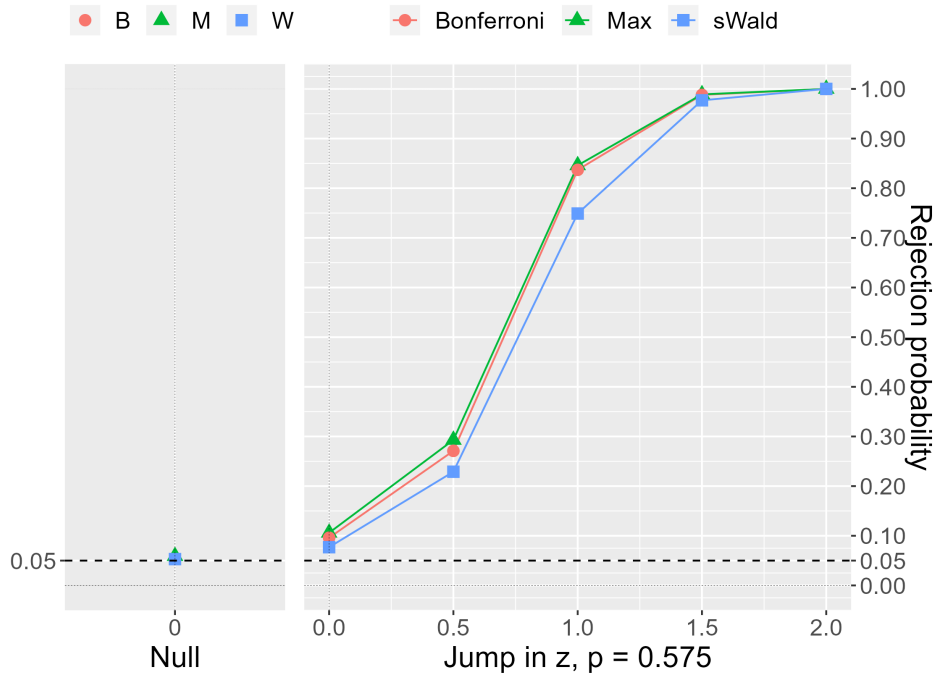


(b) Covariates have the same pairwise correlation coefficient of 0.3

Figure 9: A jump in the three covariates with a density,  $n = 1000$

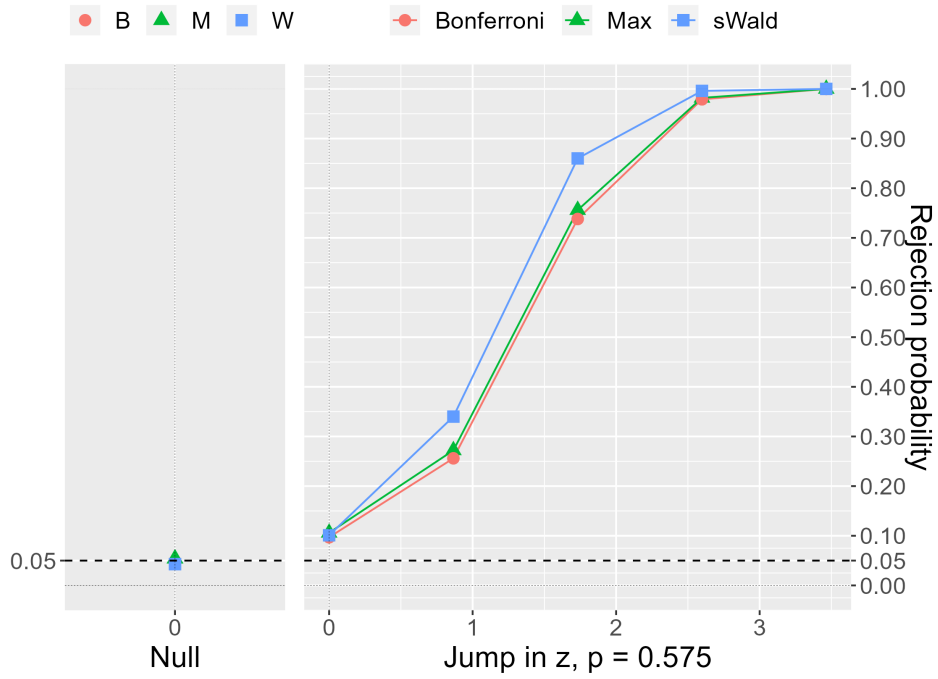


(a) Covariates have the same pairwise correlation coefficient of 0

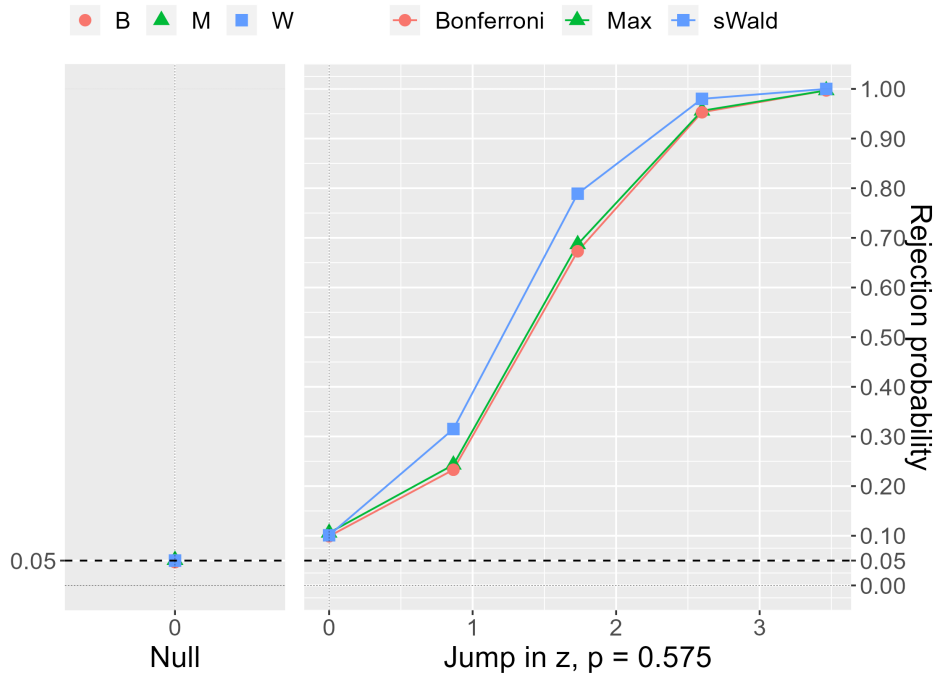


(b) Covariates have the same pairwise correlation coefficient of 0.3

Figure 10: A jump in the five covariates with a density,  $n = 1000$

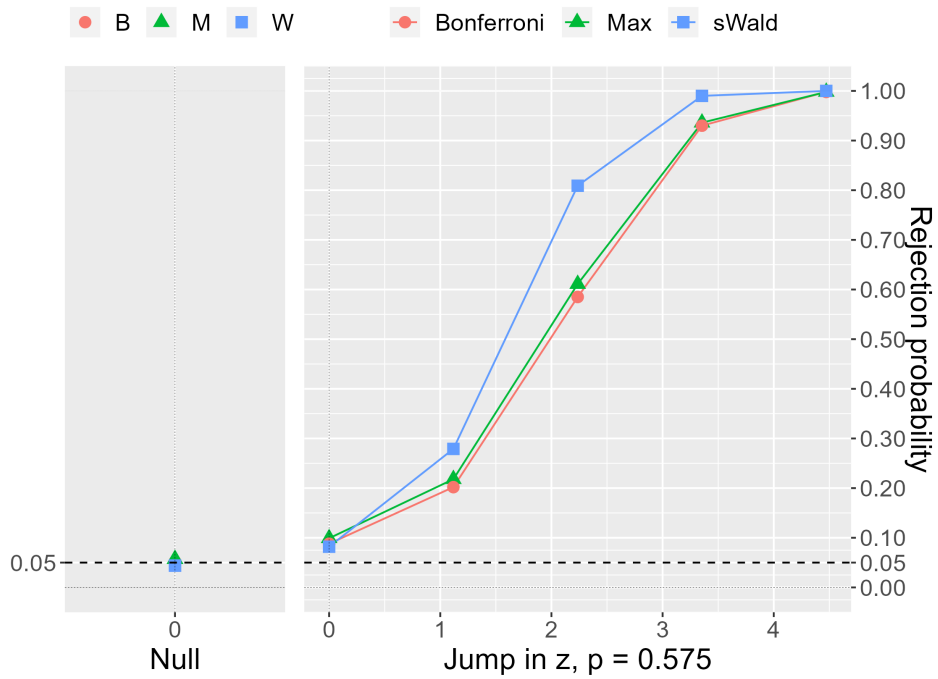


(a) Covariates have the same pairwise correlation coefficient of 0

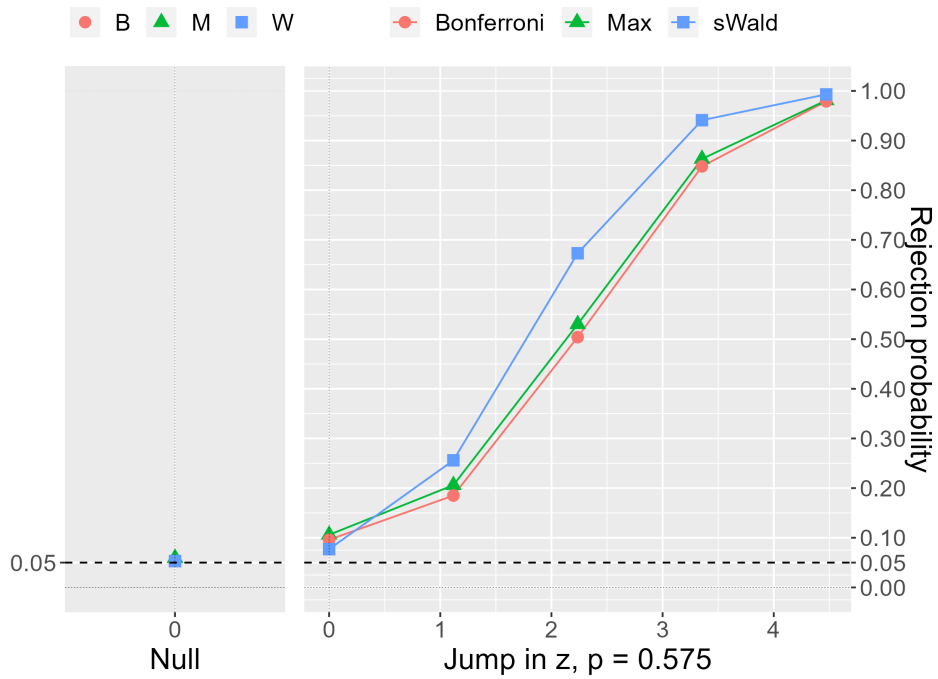


(b) Covariates have the same pairwise correlation coefficient of 0.3

Figure 11: 1/3 of jumps in all the three covariates with a density,  $n = 1000$ .



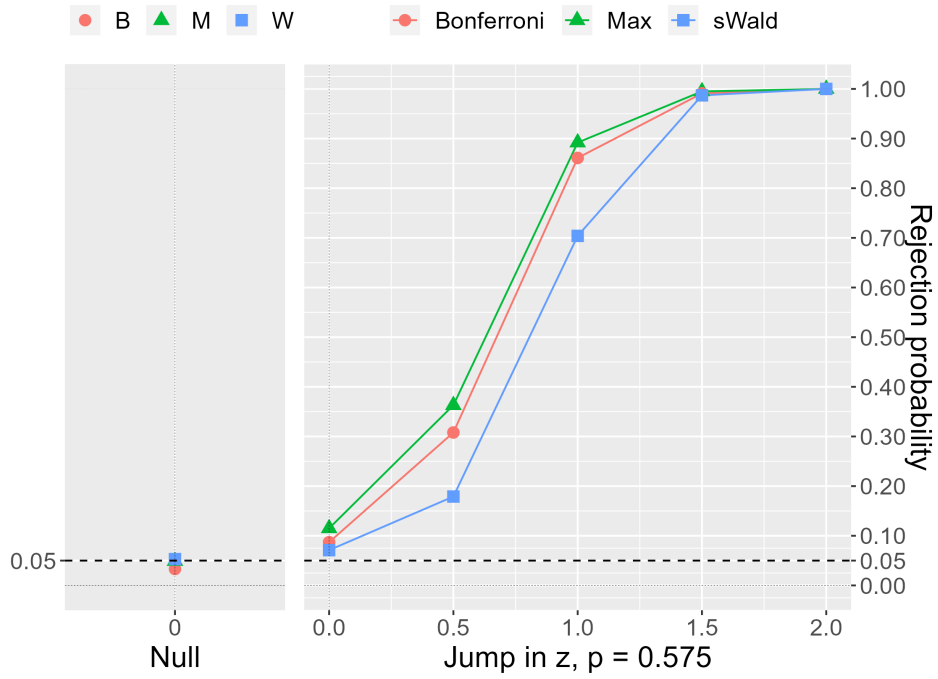
(a) Covariates have the same pairwise correlation coefficient of 0



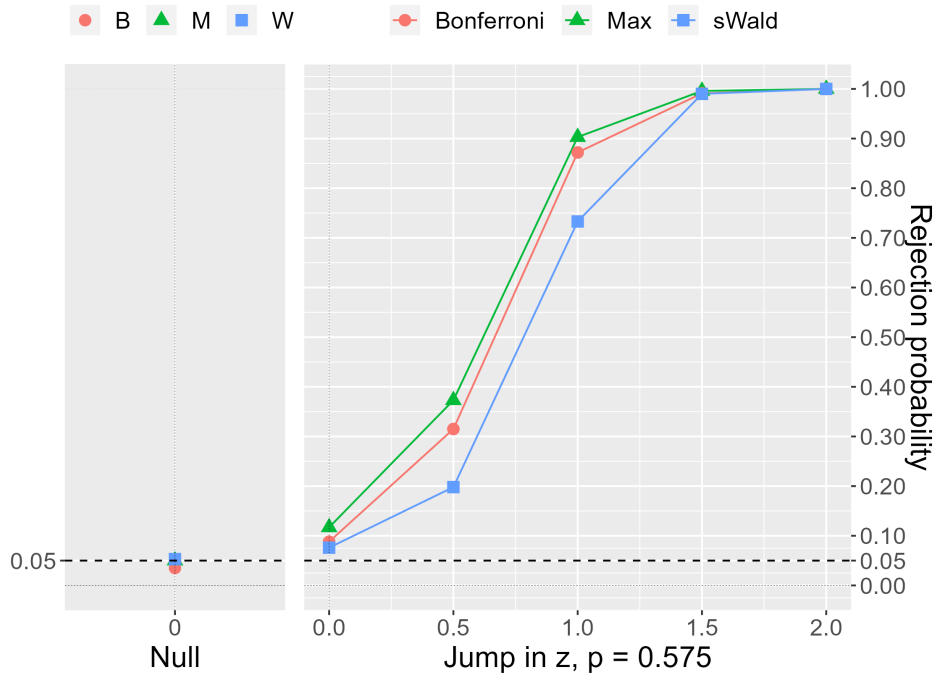
(b) Covariates have the same pairwise correlation coefficient of 0.3

Figure 12: 1/5 of jumps in all the five covariates with a density,  $n = 1000$ .



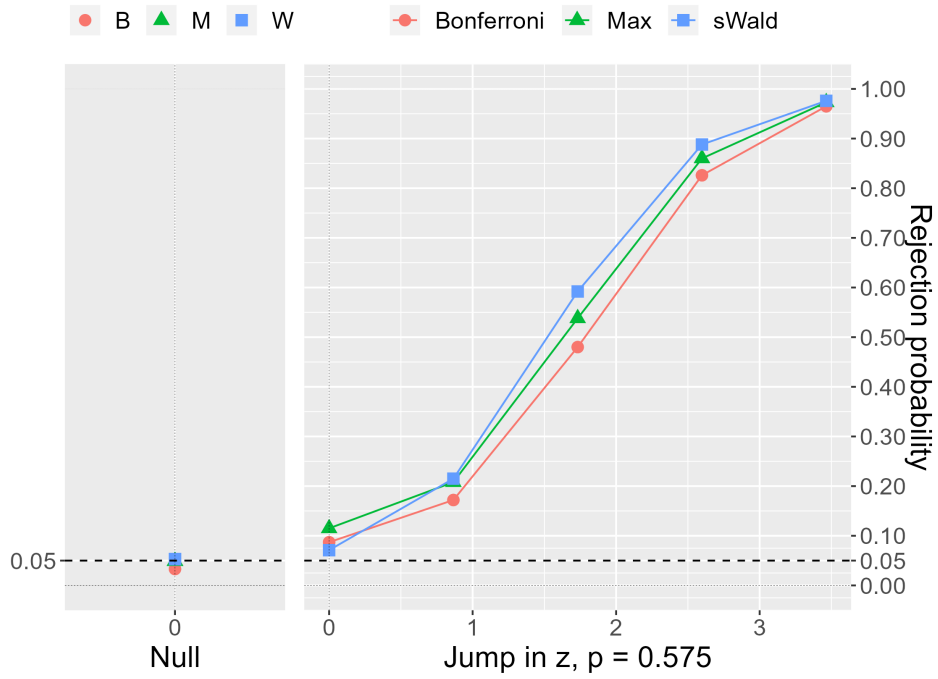


(a) The remaining one has the same pairwise correlation coefficient of 0.9.

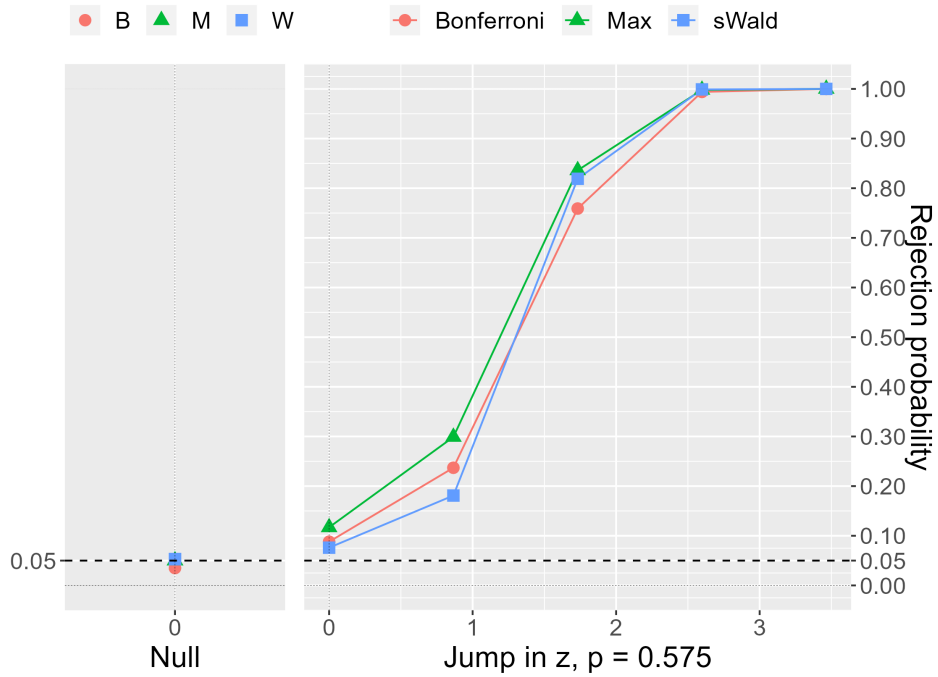


(b) The remaining one has the pairwise correlation coefficient of  $-0.9$ .

Figure 13: A jump in the three covariates with a density,  $n = 1000$ . Two out of three covariates have the same pairwise correlation coefficient of 0.9



(a) The remaining one has the same pairwise correlation coefficient of 0.9.



(b) The remaining one has the pairwise correlation coefficient of  $-0.9$ .

Figure 14: 1/3 of jumps in all the three covariates with a density,  $n = 1000$ . Two out of three covariates have the same pairwise correlation coefficient of 0.9

## References

- ABDULKADIROĞLU, A., J. ANGRIST, AND P. PATHAK (2014): “The Elite Illusion: Achievement Effects at Boston and New York Exam Schools,” *Econometrica*, 82, 137–196.
- BUGNI, F. A. AND I. A. CANAY (2021): “Testing Continuity of a Density via g-order Statistics in the Regression Discontinuity Design,” *Journal of Econometrics*, 221, 138–159.
- CALONICO, S., M. D. CATTANEO, AND M. H. FARRELL (2020): “Optimal bandwidth choice for robust bias-corrected inference in regression discontinuity designs,” *The Econometrics Journal*, 23, 192–210.
- (2022): “Coverage error optimal confidence intervals for local polynomial regression,” *Bernoulli*, 28, 2998–3022.
- CALONICO, S., M. D. CATTANEO, M. H. FARRELL, AND R. TITIUNIK (2017): “Rdrobust: Software for Regression-discontinuity Designs,” *The Stata Journal*, 17, 372–404.
- CALONICO, S., M. D. CATTANEO, AND R. TITIUNIK (2014): “Robust Nonparametric Confidence Intervals for Regression-Discontinuity Designs,” *Econometrica*, 82, 2295–2326.
- (2015): “Optimal data-driven regression discontinuity plots,” *Journal of the American Statistical Association*, 110, 1753–1769.
- CANAY, I. A. AND V. KAMAT (2018): “Approximate Permutation Tests and Induced Order Statistics in the Regression Discontinuity Design,” *The Review of Economic Studies*, 85, 1577–1608.
- CATTANEO, M. D., B. R. FRANSEN, AND R. TITIUNIK (2015): “Randomization Inference in the Regression Discontinuity Design: An Application to Party Advantages in the U.S. Senate,” *Journal of Causal Inference*, 3, 1–24.
- CATTANEO, M. D., N. IDROBO, AND R. TITIUNIK (2019): *A Practical Introduction to Regression Discontinuity Designs: Foundations*, Cambridge University Press.

- (2023): “A Practical Introduction to Regression Discontinuity Designs: Extensions,” *arXiv:2301.08958 [econ, stat]*.
- CATTANEO, M. D., M. JANSSON, AND X. MA (2018): “Manipulation testing based on density discontinuity,” *The Stata Journal*, 18, 234–261.
- (2020): “Simple local polynomial density estimators,” *Journal of the American Statistical Association*, 115, 1449–1455.
- CATTANEO, M. D., R. TITIUNIK, AND G. VAZQUEZ-BARE (2016): “Inference in Regression Discontinuity Designs under Local Randomization,” *The Stata Journal*, 16, 331–367.
- DI NARDO, J. AND D. S. LEE (2011): *Chapter 5 - Program Evaluation and Research Designs In O. Ashenfelter and D. Card (Ed.). Handbook of Labor Economics*, Elsevier, vol. 4, 463–536.
- DURRETT, R. (2019): *Probability: theory and examples*, vol. 49, Cambridge university press.
- FAN, J. AND I. GIJBELS (1996): *Local polynomial modelling and its applications: monographs on statistics and applied probability 66*, vol. 66, CRC Press.
- FORT, M., A. ICHINO, AND G. ZANELLA (2020): “Cognitive and Noncognitive Costs of Day Care at Age 0–2 for Children in Advantaged Families,” *Journal of Political Economy*, 128, 158–205.
- HAHN, J., P. TODD, AND W. V. DER KLAUW (2001): “Identification and Estimation of Treatment Effects with a Regression-Discontinuity Design,” *Econometrica*, 69, 201–209.
- IMBENS, G. W. AND T. LEMIEUX (2008): “Regression discontinuity designs: A guide to practice,” *Journal of Econometrics*, 142, 615–635.
- ISHIHARA, T. AND M. SAWADA (2023): “Manipulation-Robust Regression Discontinuity Designs,” *arXiv:2009.07551 [econ, stat]*.
- JOHNSON, M. S. (2020): “Regulation by Shaming: Deterrence Effects of Publicizing Violations of Workplace Safety and Health Laws,” *American Economic Review*, 110, 1866–1904.

- KORTING, C., C. LIEBERMAN, J. MATSUDAIRA, Z. PEI, AND Y. SHEN (2023): “Visual Inference and Graphical Representation in Regression Discontinuity Designs,” *The Quarterly Journal of Economics*, qjad011.
- LEE, D. S. (2008): “Randomized Experiments from Non-Random Selection in U.S. House Elections,” *Journal of Econometrics*, 142, 675–697.
- LEE, D. S. AND T. LEMIEUX (2010): “Regression Discontinuity Designs in Economics,” *Journal of Economic Literature*, 48, 281–355.
- MCCRARY, J. (2008): “Manipulation of the Running Variable in the Regression Discontinuity Design: A Density Test,” *Journal of Econometrics*, 142, 698–714.
- MEYERSSON, E. (2014): “Islamic Rule and the Empowerment of the Poor and Pious,” *Econometrica*, 82, 229–269.
- OTSU, T., K.-L. XU, AND Y. MATSUSHITA (2013): “Estimation and Inference of Discontinuity in Density,” *Journal of Business & Economic Statistics*, 31, 507–524.
- SERFLING, R. J. (1980): *Approximation theorems of mathematical statistics*, John Wiley & Sons.
- VAN DER VAART, A. W. AND J. A. WELLNER (1996): *Weak convergence and empirical processes*, Springer New York, NY.